Altered protein expression of membrane transporters in isolated cerebral microvessels and brain cortex of a rat Alzheimer's disease model

Puris, E.; Auriola, S.; Petralla, S.; Hartman, R.; Gynther, M.; Lange, E.C.M. de; Fricker, G.

Neurobiology of Disease 169 (2022) 105741

Contents lists available at ScienceDirect

Neurobiology of Disease

journal homepage: www.elsevier.com/locate/ynbdi

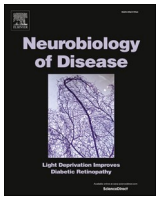

Altered protein expression of membrane transporters in isolated cerebral microvessels and brain cortex of a rat Alzheimer's disease model

Elena Puris [a,*], Seppo Auriola [b], Sabrina Petralla [a], Robin Hartman [c], Mikko Gynther [a], Elizabeth C.M. de Lange [c], Gert Fricker [a]

[a] Institute of Pharmacy and Molecular Biotechnology, Ruprecht-Karls-University, Im Neuenheimer Feld 329, 69120 Heidelberg, Germany
[b] School of Pharmacy, University of Eastern Finland, P.O. Box 1627, 70211 Kuopio, Finland
[c] Predictive Pharmacology Group, Division of Systems Biomedicine and Pharmacology, Leiden Academic Centre for Drug Research, Leiden University, the Netherlands

ARTICLE INFO

Keywords:
Brain microvessels
Brain cortex
Alzheimer's disease (AD)
Solute carrier (SLC) transporters
ATP-binding cassette (ABC) transporters
Animal model

ABSTRACT

There is growing evidence that membrane transporters expressed at the blood-brain barrier (BBB) and brain parenchymal cells play an important role in Alzheimer's disease (AD) development and progression. However, quantitative information about changes in transporter protein expression at neurovascular unit cells in AD is limited. Here, we studied the changes in the absolute protein expression of five ATP-binding cassette (ABC) and thirteen solute carrier (SLC) transporters in the isolated brain microvessels and brain cortical tissue of TgF344-AD rats compared to age-matched wild-type (WT) animals using liquid chromatography tandem mass spectrometry based quantitative targeted absolute proteomic analysis. Moreover, sex-specific alterations in transporter expression in the brain cortical tissue of this model were examined. Protein expressions of Abcg2, Abcc1 and FATP1 (encoded by Slc27a1) in the isolated brain microvessels of TgF344-AD rats were 3.1-, 2.0-, 4.3-fold higher compared to WT controls, respectively ($p < 0.05$). Abcc1 and 4F2hc (encoded by Slc3a2) protein expression was significantly up-regulated in the brain cortical tissue of male TgF344-AD rats compared to male WT rats ($p < 0.05$). The study provides novel information for the elucidation of molecular mechanisms underlying AD and valuable knowledge about the optimal use of the TgF344-AD rat model in AD drug development and drug delivery research.

1. Introduction

Alzheimer's disease (AD) is a progressive neurodegenerative disease with an alarming increase in incidence over the last years (Alzheimer's Association, 2016). At present, there is no treatment available to cure or to slow the AD progression, which is mainly due to the limitations of current knowledge about the disease pathogenesis (Mehta et al., 2017). The extensive research on AD has so far revealed several hallmarks of the disease, such as presence of extracellular amyloid-β (Aβ) plaques, deposition of Aβ in cerebral medium-sized and microvessels, known as

Abbreviations: Aβ, amyloid-β; ABC, ATP-binding cassette transporter; AD, Alzheimer's disease; APP, β-amyloid precursor protein; ASCT1, alanine/serine/cysteine/threonine transporter 1,; BACE1, β-site APP cleaving enzyme 1; BBB, blood-brain barrier; BCRP/Bcrp, human/rodent breast cancer resistance protein; CAA, cerebral amyloid angiopathy; CAT-1, cationic amino acid transporter 1; CERP/Cerp, human/rodent cholesterol efflux regulatory protein; COX2, Cyclooxygenase-2; DHA, docosahexaenoic acid; ECs, endothelial cells; ENT1, equilibrative nucleoside transporter 1; FAD, familial Alzheimer's disease; FATP1, fatty acid transport protein 1; γ-Gtp, γ-glutamyltransferase; Gapdh, glyceraldehyde-3-phosphate dehydrogenase; Gfap, glial fibrillary acidic protein; GLUT1, glucose transporter 1; HPLC, high-performance liquid chromatography; Il1a, Interleukin-1 alpha; Il1b, Interleukin-1 beta; LAT1, large neutral amino acids transporter small subunit 1; MCT1, monocarboxylate transporter 1; MDR1/Mdr1, human/ rodent multidrug resistance protein 1; MRM, multiple reaction monitoring; MRP1/Mrp1, human/ rodent multidrug resistance-associated protein 1; NFT, neurofibrillary tangles; NVU, neurovascular unit; OATP, organic anion-transporting polypeptide; OAT1, organic anion transporter 1; OCT1, organic cation transporter 1; PC, phosphatidylcholine; Pdgfrb, platelet-derived growth factor receptor beta; Pecam1, platelet and endothelial cell adhesion molecule 1; PSEN, presenilin; ROS, reactive-oxygen species; QTAP, quantitative targeted absolute proteomics; RFC, reduced folate transporter; SAD, sporadic Alzheimer's disease; SLC -, solute carrier transporter; Syp -, synaptophysin; HPLC-MS/MS, high-performance liquid chromatography tandem mass spectrometry; WT, wild-type; 4F2hc, 4F2 cell-surface antigen heavy chain..

* Corresponding author at: Institute of Pharmacy and Molecular Biotechnology, Ruprecht-Karls-University, Im Neuenheimer Feld 329, 69120 Heidelberg, Germany.
E-mail address: elena.puris@uni-heidelberg.de (E. Puris).

https://doi.org/10.1016/j.nbd.2022.105741
Received 6 January 2022; Received in revised form 25 March 2022; Accepted 20 April 2022
Available online 25 April 2022

cerebral amyloid angiopathy (CAA), accumulation of intracellular aggregates of hyperphosphorylated tau protein, neurodegeneration, synaptic loss, inflammatory reaction, alteration in metabolic pathways and lipid metabolism (Guo et al., 2020; Heneka et al., 2015). All these mechanisms lead to irreversible degeneration of the brain resulting in memory and cognition impairment followed by the death from brain failure. The familial form of AD (FAD) is caused by mutations in the genes involved in Aβ production, i.e. presenilin 1 and 2 (PSEN1 and PSEN2) or β-amyloid precursor protein (APP). The knowledge about the mechanisms underlying the development and progression of the more common (95% of all cases) AD form - sporadic AD (SAD), is still limited. Interestingly, two-thirds of the AD patients are women (Laws et al., 2018). Large population studies displays that women are at greater risk of developing the disease, and show faster cognitive decline after diagnosis of AD dementia (Ferretti et al., 2018; Gao et al., 1998; Laws et al., 2018). Although sex-specific discrepancies in underlying AD pathology have been found (Filon et al., 2016; Malpetti et al., 2017), the molecular mechanisms behind the differences in AD manifestation and progression between men and women are unknown.

The blood-brain barrier (BBB) is a crucial physical and biochemical barrier for controlling brain homeostasis and regulating blood-to-brain flux of endogenous and exogenous compounds including drugs. The BBB is primarily formed by the brain microvascular endothelial cells (ECs), which protective function is attributed to the presence of tight junctions between the ECs, expression of metabolizing enzymes, and membrane transporters (Kadry et al., 2020). However, the "barrier" characteristics of the brain microvascular ECs is achieved by highly-regulated cell-cell communication with glial cells (i.e., astrocytes, microglia), pericytes that share the same basement membrane as the ECs, neurons initially observed in brain capillary beds, and extracellular matrix (Menaceur et al., 2021). All these cells, including ECs, form the neurovascular unit (NVU). The NVU and particularly the BBB have been shown to be disrupted in AD (Liu et al., 2019; Sweeney et al., 2018). The resulting disturbance of the protective function of the BBB is thought to be one of the causes and consequences of AD (Erickson and Banks, 2013). The BBB dysfunction in AD leads to the altered transport of essential nutrients to the brain, impaired clearance of metabolites across the BBB, entry of toxic blood-derived compounds, cells, and pathogens to the AD brain followed by inflammatory and immune responses associated with multiple neurodegenerative pathways (Erickson and Banks, 2013).

The membrane transporters expressed at the cells of the NVU play important roles in mediating the influx (mainly Solute carrier family transporters, or SLCs) and efflux (mainly adenosine triphosphate (ATP)-binding cassette transporters, or ABCs) of solutes, including nutrients, metabolites and drugs, across the BBB and the membranes of the brain parenchymal cells (Abbott et al., 2010). There is growing evidence that ABC and SLC transporters expressed at the NVU cells play a key role in AD pathogenesis by contributing to several molecular pathways involved in the disease progression (Jia et al., 2020; Pereira et al., 2018). For instance, ABCB1 (also known as multidrug resistance protein 1, MDR1) is responsible for the clearance of Aβ from the brain, and its reduced function at the BBB in AD patients can be one of the reasons of extracellular Aβ accumulation in the brain (Chai et al., 2020; van Assema et al., 2012). In addition, there is mounting evidence that other transporters, such as ABCG2 (also known as breast cancer resistance protein, BCRP), ABCC1 (also known as multidrug resistance-associated protein 1, MRP1) and ABCA1 (also known as cholesterol efflux regulatory protein, CERP), are involved in Aβ transport across the BBB (Jia et al., 2020; Pereira et al., 2018). SLC transporters, such as those encoded by SLC2A1, SlC7A1, SLC7A5, SLC16A1, SLC19A1, SLCO1A2, SLCO1C1, SLC22A1, SLC22A6, SLC22A8, SLC27A1, SLC29A1, can play a potential role in AD pathogenesis, as their function and/or expression were shown to be altered in AD brains or preclinical models of AD (Al-Majdoub et al., 2019; Czapiga and Colton, 2003; Dobryakova et al., 2019; Furst and Lal, 2011; Jia et al., 2020; Lyros et al., 2014; Ochiai et al., 2019; Robinson et al., 2018; Roostaei et al., 2017; Wittmann et al., 2015). The changes in transporter expression and function in the cells of the NVU can result in biochemical perturbations in AD as well as altered drug delivery to the brain and distribution within the brain, thereby contributing to consequent clinical outcome. There is limited information about the changes in transporter expression in the cells of the NVU in AD brains and animal models of the disease. Moreover, sex-related differences in transporter expression in AD have not been yet studied. Therefore, the investigation of changes in transporter protein expression in the NVU cells in AD with particular focus on sex-specific differences is important for development of effective AD treatments.

Animal models are essential for the identification of the molecular mechanisms underlying the progression of the disease, validating drug targets, and testing therapeutic interventions. Animal models of AD have been designed to reproduce the simplified disease phenotype with a focus on AD-related histopathological lesions and the utilization of FAD-associated genetic mutations, assuming that the events occurring after the initial trigger are the same in SAD and FAD (Guo and Zhou, 2018). TgF344-AD rat model expressing mutant human APP_{sw} and PS1ΔE9 genes provides several advantages over the mice expressing the same mutant human transgenes (Cohen et al., 2013). TgF344-AD rats manifest the full array of AD pathological features, such as age-dependent accumulation of cerebral Aβ, CAA, tauopathy, gliosis, apoptotic loss of neurons, and cognitive disturbance (Cohen et al., 2013). However, the model has not been characterized in terms of the changes in transporter protein expression at the BBB and brain parenchymal cells.

Quantitative targeted absolute proteomics (QTAP) approach has been extensively used to measure the expression of transporters, receptors, enzymes and other proteins in health and disease (Al-Majdoub et al., 2019; Ohtsuki et al., 2011; Pan et al., 2018, 2019; Puris et al., 2021; Uchida et al., 2013). The LC-MS/MS-based QTAP analysis provides a highly sensitive and robust quantification of target proteins and confers several advantages over the conventionally used antibody-based methods (Aebersold et al., 2013). The aim of the present study was to investigate AD-related changes in protein expression of ABC and SLC transporters in the isolated brain microvessels and the brain cortical tissue in TgF344-AD rats versus age-matched wild-type (WT) animals. In addition, we investigated sex-specific changes in transporter protein expression in the brain cortical tissue of TgF344-AD rats compared to WT animals. Finally, we compared the changes in transporter expression in the isolated brain microvessels and brain cortex in the rat AD model to the previously reported findings in AD patients to evaluate the relevance of the model to mimic AD-related alterations in transporter expression in humans.

2. Materials and methods

2.1. Materials

Acetonitrile, ethylenediaminetetraacetic acid (EDTA), dithiothreitol, urea, guanidine hydrochloride, Tris-HCl, formic acid and protease inhibitor cocktail were purchased from Sigma-Aldrich (St. Louis, MO). Proteome Extraction Kit was purchased from Merck KGaA, Darmstadt, Germany. The absolute quantified stable-isotope labelled peptides were purchased from JPT Peptide Technologies GmbH (Berlin, Germany). Protease-Max surfactant, tosylphenylalanylchloromethyl ketone-treated trypsin and lysyl endopeptidase (LysC) were purchased from Promega (Madison, WI, USA).

2.2. Animals

Heterozygous TgF344-AD rats expressing mutant human APP_{sw} and PS1ΔE9 genes ($n = 14$) (Cohen et al., 2013) and their age-matched WT Fischer344 counterparts ($n = 13$) were used in this study. Among the animals, there were female ($n = 6$) and male ($n = 8$) TgF344-AD rats, as

well as female ($n = 5$) and male (n = 8) WT rats. The rats were purchased from the Rat Resource & Research Center (RRRC) of the University of Missouri (Columbia, MO) and bred in the Animal Research Facility of Leiden University by the Predictive Pharmacology group of Prof. Elizabeth C.M. de Lange. The animal age of 42–44 weeks was chosen because at this time the TgF344-AD rats develop a full range of AD pathological features (Cohen et al., 2013). Information about the individual weight and age of the animals is presented in Additional file 1. The animals were housed in social groups (4 males or 5 females per cage) maintained on a 12-h light/dark cycle in a temperature-controlled environment (at a constant temperature of 21 ± 1 °C) with free access to food (Laboratory chow, Special Diets Services, Tecnilab BMI, Someren, the Netherlands) and water. All animal experiments complied with the ARRIVE guidelines and were carried out in accordance with the EU Directive 2010/63/EU for animal experiments and Dutch laws on animal experimentation. All procedures were approved by the Ethics Committee for Animal Experiments of Leiden University (AVD1060020171766).

2.3. Sample collection

Animals were killed by means of carbon dioxide asphyxiation. Rats were transcardially perfused with Tris-buffered saline to remove the blood. The brains were excised, the cerebrums were extracted and transferred to ice cold buffer A (101 mM NaCl, 4.6 mM KCl, 5 mM $CaCl_2{\cdot}2H_2O_2$, 1.2 mM KH_2PO_4, 1.2 mM $MgSO_4{\cdot}7H_2O$, 15 mM HEPES; pH 7.4) for the immediate microvessel isolation. The part of the prefrontal cortex (ca. 15 mg) was collected, snap frozen and stored at −80 °C until the LC-MS/MS proteomics analysis (section 2.7), Aβ ELISA assays (section 2.4) or gene quantification (section 2.5).

2.4. Aβ ELISA assays

The total levels of $A\beta_{1–40}$ and $A\beta_{1–42}$ were analysed by ELISA from freshly frozen cortical samples. The brain cortical samples (100 mg) were homogenized in 800 μL of guanidine buffer (5 mM guanidine-HCl/50 mM Tris-HCl, pH 8) followed by dilution with DPBS containing complete inhibitory mixture (Roche Diagnostics, Mannheim, Germany) according to previously published protocol (Oakley et al., 2006). Samples were centrifuged for 20 min at 16000 ×*g* at 4 °C. Supernatant was taken for analysis of Aβ. The levels of $A\beta_{40}$ and $A\beta_{42}$ were measured using Human $A\beta_{40}$ and $A\beta_{42}$ ELISA Kits (Thermo Fisher Scientific, KHB3481 for $A\beta_{40}$ and KHB3544 for $A\beta_{42}$), following the manufacturer's instructions. The levels of $A\beta_{1–40}$ and $A\beta_{1–42}$ were standardized to brain tissue weight and expressed as micrograms of Aβ per gram (wet brain cortical tissue). The data are presented as mean ± SEM.

2.5. Quantitative real-time polymerase chain reaction (qRT-PCR)

Quantitative real-time polymerase chain reaction (qRT-PCR) analysis was used for quantification of gene expression of inflammation markers, such as Cyclooxygenase-2 (COX2) and inflammatory cytokines, Interleukin-1 alpha (Il1a) and 1 beta (Il1b) in brain cortical tissues of WT and TgF344-AD rats. In addition, qRT-PCR was performed for demonstration of enrichment and purity of the isolated brain microvessels by quantification of the gene expression of cell-specific markers in the isolated brain microvessels vs. the corresponding brain cortical tissue (Section 2.6). First, total RNA was extracted from brain cortical tissue of WT and TgF344-AD rats using the RNeasy Mini Kit (Qiagen, Stockach, Germany) according to the manufacturer's instructions and quantified by a NanoDrop (Thermo Scientific, Dreieich, Germany). Subsequently, cDNA was synthetized using iScriptTM cDNA synthesis kit (Bio-Rad Laboratories, Munich, Germany) according to the manufacturer's protocol. Total RNA (1 μg) was used as template for reverse transcription in 20 μL reaction volumes and then diluted with RNase-free water. After that, the synthesized cDNA was mixed with the PowerUp SYBR Green MasterMix (Life Technologies) and various sets of gene-specific primers (Table S1) validated previously (Peinnequin et al., 2004) and purchased from (ThermoFisher Scientific). Normalized relative expression per sample was calculated by dividing the relative quantity of a given target/sample by the geometric mean of the relative quantities of housekeeping gene glyceraldehyde-3-phosphate dehydrogenase (Gapdh) according to Taylor et al. (2019) (Taylor et al., 2019). The qRT-PCR was performed using a LightCycler 96 (Roche Diagnostics), data were acquired using LightCycler® 96 SW 1.1 software, v. 1.1.0.1320 (Roche Diagnostics, Mannheim, Germany; 2011).

2.6. Brain microvessel isolation

Rat brain microvessels were isolated by a combination of dextran density gradient separation and size filtration according to the published validated protocols with minor modifications (Al-Majdoub et al., 2019; Hoshi et al., 2013). This isolation method is commonly used for LC-MS/MS-based QTAP analyses of the transporter protein expression in human and animal models. All isolation procedures were carried out at 4 °C. Two rat cortices (approximately 3 g) were dissected into 1 mm pieces and homogenized using the Dounce homogenizer with 20 up-and-down, unrotated strokes in five volumes of buffer A per tissue weight (g). The homogenate was centrifuged at 2000 ×*g* for 10 min at 4 °C. The resulting pellet was suspended in buffer B (buffer A containing 16% dextran). The suspension was centrifuged at 4500 ×*g* for 15 min at 4 °C. The supernatant was transferred to a new tube, and centrifuged again at 4500 ×*g* for 15 min at 4 °C. The two resulting pellets were suspended and mixed in buffer C (buffer A containing 5 g/L bovine serum albumin). The obtained suspension was passed through a 200 μm nylon mesh, followed by the mesh wash with 10 mL of buffer C. The resulting suspension was passed through a 100 μm nylon mesh, followed by the mesh wash with 10 mL of buffer C. The suspension passing through the 100 μm nylon mesh was loaded onto 20 μm nylon mesh. The brain medium-sized vessels retained on the 100 μm nylon mesh were immediately collected by diverting the 100 μm nylon mesh and washing the mesh with buffer C (30 mL). Subsequently, the mesh was washed with 40 mL of buffer C. The brain microvessels retained on the 20 μm nylon mesh were immediately collected by diverting the 20 μm nylon mesh and washing the mesh with buffer C (30 mL). The suspension containing the brain microvessels and medium-sized vessels was centrifuged at 1000 ×*g* for 5 min at 4 °C. After discarding the supernatant, the pellet was suspended in 1 mL of buffer A. The suspension obtained after centrifugation of the brain medium-sized was centrifuged at 1000 ×*g* for 5 min at 4 °C. After complete removal of the supernatant, the pellet was snap frozen and stored at −80 °C until the western blot analysis as described below. The suspension obtained after centrifugation of the brain microvessels was used to observe the brain capillaries through a microscope. Finally, the suspension was centrifuged at 1000 ×*g* for 5 min at 4 °C, and the supernatant was completely removed. The pellet was used for crude membrane fraction isolation as described below.

The enrichment and purity of the isolated brain microvessel fraction were evaluated microscopically as described above. In addition, to confirm the enrichment and purity of the isolated brain microvessels, the gene expression of cell-specific marker of ECs, platelet and endothelial cell adhesion molecule 1 (Pecam1); astrocyte marker, glial fibrillary acidic protein (Gfap); pericyte marker, platelet-derived growth factor receptor beta, (Pdgfrb); neuronal marker, synaptophysin (Syp), were measured using qRT-PCR in freshly isolated brain microvessels or corresponding brain cortical tissue from three wild-type rats. The qRT-PCR analysis was performed in a similar way as discussed in section 2.5 using gene-specific primers (Table S1) purchased from (ThermoFisher Scientific). In addition, the purity of the brain microvessel preparations was evaluated by measuring the protein expression levels of the plasma membrane marker Na^+/K^+-ATPase localized on abluminal membrane of brain capillaries and the endothelial marker γ-glutamyltransferase (γ-Gtp) localized on luminal membrane of brain capillaries

(Cornford and Hyman, 2005).

2.7. Quantitative targeted absolute proteomic analysis

The absolute protein expression levels of ABC and SLC transporters (Table 1) as well as plasma membrane marker Na^+/K^+-ATPase and endothelial cell marker γ-Gtp were quantified in crude membrane fraction of the rat brain cortices and isolated brain microvessels. The following transporters with potential or proven role in AD were selected for the quantification: Abcb1a/b (Mdr1a/b), Abcg2 (Bcrp), Abcc1 (Mrp1), Abcc4 (Mrp4), Abca1 (Cerp), alanine/serine/cysteine/threonine transporter 1 (ASCT1, encoded by Slc1a4), facilitated glucose transporter member 1 (GLUT1, encoded by Slc2a1), large neutral amino acids transporter small subunit 1 (LAT1, encoded by Slc7a5) and 4F2 cell-surface antigen heavy chain (4F2hc, encoded by Slc3a2), high affinity cationic amino acid transporter 1 (CAT-1/Slc7a1), monocarboxylate transporter 1 (MCT1, encoded by Slc16a1), reduced folate transporter (RFC/Slc19a1), organic anion-transporting polypeptide 1a4 (OATP1A4, encoded by Slco1a4), a rat ortholog of human OATP1A2 (encoded by SLCO1A2), organic anion-transporting polypeptide 1C1 (OATP1C1, encoded by Slco1c1), organic cation transporter 1 (OCT1, encoded by Slc22a1), organic anion transporter 1 (OAT3, encoded by Slc22a8), fatty acid transport protein 1 (FATP1, encoded by Slc27a1), equilibrative nucleoside transporter 1 (ENT1, encoded by Slc29a1) (Al-Majdoub et al., 2019; Czapiga and Colton, 2003; Dobryakova et al., 2019; Furst and Lal, 2011; Jia et al., 2020; Lyros et al., 2014; Ochiai et al., 2019; Pereira et al., 2018; Robinson et al., 2018; Roostaei et al., 2017; Wittmann et al., 2015). The crude membrane fractions were isolated using ProteoExtract Subcellular Proteome Extraction Kit (Merck KGaA, Darmstadt, Germany) according to the manufacturer's instructions. After measuring total protein concentrations in the crude membrane fraction by the Bio-Rad DC Protein Assay, the samples were

Table 1
Probe peptide amino acid sequences and multiple reaction monitoring transitions for the LC-MS/MS analysis of target proteins.

Protein/gene name	St/IS	Unique amino acid sequence	Retention time (min)	MRM transitions (*m/z*)				
				Q1	Q3.1	Q3.2	Q3.3	Q3.4
ABC transporters								
Abcb1/Abcb1[a]	St	NTTGALTTR	8.7	467.7	719.4	618.3	561.3	
	IS	NTTGALTT**R***	8.7	472.7	729.4	628.3	517.3	
Abcg2Abcg2	St	SSLLDVLAAR	27.7	522.8	757.4	644.3	529.3	
	IS	SSLLDVLAA**R***	27.7	527.8	767.4	654.3	539.3	
Abcc1/Abcc1	St	TPSGNLVNR	9.7	479.2	759.4	672.3	501.3	
	IS	TPSGNLVN**R***	9.7	484.2	769.4	682.3	511.3	
Abcc4/Abcc4	St	APVLFFDR	24.8	482.7	796.4	697.3	584.2	
	IS	APVLFFD**R***	24.8	487.7	806.4	707.3	594.2	
Abca1/Abca1	St	FVSPLSWDLVGR	30.2	688.4	1129.6	1042.6	247.1	
	IS	FVSPLSWDLVG**R***	30.2	693.4	1139.6	1052.6	247.1	
SLC transporters								
ASCT1/ Slc1a4	St	ETVDSFLDLLR	32.5	654.3	1077.6	978.5	863.5	776.5
	IS	ETVDSFLDLL**R***	32.5	659.3	1087.6	988.5	873.5	786.5
GLUT1/Slc2a1	St	TFDEIASGFR	21.4	571.7	894.4	779.4	650.4	537.3
	IS	TFDEIASGF**R***	21.4	576.7	904.4	789.4	660.4	547.3
4F2hc/Slc3a2	St	VAGSPGWVR	14.6	464.7	829.4	758.4	701.4	614.3
	IS	VAGSPGWV**R***	14.6	469.7	839.4	768.4	711.4	624.3
CAT-1/Slc7a1	St	TILSPK	11.7	329.7	557.4	444.4	331.2	
	IS	TILSP**K***	11.7	333.7	565.4	452.4	339.2	
LAT1/Slc7a5	St	VQDAFAAAK	12.1	460.7	821.4	578.3	507.3	
	IS	VQDAFAAA**K***	12.1	464.8	829.4	586.3	515.3	
MCT1/Slc16a1	St	SITVFFK	23.5	421.3	641.4	441.2	294.2	
	IS	SITVFF**K***	23.5	425.3	649.4	449.2	302.2	
RFC/Slc19a1	St	DSFLVR	17.0	368.7	534.3	387.3	274.2	
	IS	DSFLV**R***	17.0	373.7	544.3	397.3	284.2	
OATP1A4/ Slco1a4	St	EVATHGVR	5.0	434.7	640.4	468.3	331.2	
	IS	EVATHGV**R***	5.0	439.7	650.4	478.3	341.2	
OATP1C1/ Slco1c1	St	DFLPSLK	22.8	410.2	557.4	444.3	263.1	
	IS	DFLPSL**K***	22.8	414.2	565.4	452.3	263.1	
OCT1/Slc22a1	St	ENTIYLQVQTGK	18.2	697.4	773.5	660.4	532.3	
	IS	ENTIYLQVQTG**K***	18.2	701.4	781.5	668.4	540.3	
OAT3/Slc22a8	St	YGLSDLFR	27.1	485.8	807.4	637.3	550.3	
	IS	YGLSDLF**R***	27.1	490.8	817.4	647.3	560.3	
FATP1/Slc27a1	St	LLPQVDTTGTFK	20.5	660.4	1093.6	996.5	868.44	769.4
	IS	LLPQVDTTGTF**K***	20.5	664.4	1101.6	1004.5	876.4	777.4
ENT1/Slc29a1	St	EESGVPGPNSLPANR	15.0	762.4	1022.5	457.3	502.2	
	IS	EESGVPGPNSLPAN**R***	15.0	767.4	1032.5	467.3	502.2	
Endothelial marker, luminal membrane								
γ-Gtp	St	LFQPSIQLAR	22.4	586.8	784.4	687.4	600.4	
	IS	LFQPSIQLA**R***		591.8	794.4	697.4	610.4	
Plasma membrane marker								
Na^+/K^+–ATPase	St	AAVPDAVGK	10.8	414.3	685.4	586.3	489.3	
	IS	AAVPDAVG**K***	10.8	418.3	693.4	594.3	497.3	

Abcb1 refers to both Abcb1a and Abcb1b.
St – standard, IS – internal standard.
Bold letter with* denotes labelled arginine (R) or lysine (K) with a stable isotope ^{13}C and ^{15}N.

prepared according to previously published methods (Gynther et al., 2017; Uchida et al., 2011). Briefly, the aliquots of samples containing 50 μg of total protein were solubilized in 7 M guanidine hydrochloride, 500 mM Tris–HCl (pH 8.5) and 10 mM EDTA. The proteins were reduced with dithiothreitol and *S*-carbamoylmethylated with iodoacetamide, followed by precipitation with methanol and chloroform. The precipitates were dissolved by addition of 6 M urea in 0.1 M Tris–HCl (pH 8.5) followed by a 5-fold dilution with 0.1 M Tris–HCl (pH 8.5), which was spiked with a mixture of internal standard peptides (Table 1). This step was followed by the addition of Lys-C and Protease-Max, with subsequent incubation at room temperature for 3 h. Finally, tosylphenylalanyl chloromethyl ketone-treated trypsin was added for tryptic 16-h digestion of the samples (enzyme/substrate ratio of 1:100) at 37 °C. Formic acid in water 20% (*v*/v) was used to acidify the samples, followed by centrifugation at 14000 ×*g* for 5 min at 4 °C. The supernatants were used for LC-MS/MS analysis described below. The LC-MS/MS analysis was performed by coupling an Agilent 1290 Infinity LC (Agilent Technologies, Waldbronn, Germany) system to an Agilent 6495 Triple Quadrupole Mass Spectrometer equipped with an ESI source (Agilent Technologies, Palo Alto, CA, USA). The HPLC method using Advance Bio Peptide Map column (2.1 × 250 mm, 2.7 μm) was applied for separation and elution of peptides as described previously (Gynther et al., 2017; Gynther et al., 2018; Puris et al., 2019).

The eluted peptides were simultaneously detected using the positive ion multiple reaction monitoring (MRM) mode. The dwell time was 20 ms per transition. The source temperature was 210 °C with drying gas at a flow rate of 16 L/min. The nebulizer pressure was 45 psi and MS capillary voltage was 3 kV. The quantitation of the target protein was based on one unique peptide (Table 1) selected according to the in silico peptide selection criteria (Uchida et al., 2011) and previous reports (Gynther et al., 2017; Gynther et al., 2018; Hoshi et al., 2013; Puris et al., 2019). Three or four MRM transitions for each specific peptide related to high intensity fragment ions were selected for quantification of a stable isotope-labelled peptide and the unlabelled investigated peptide (Table 1).

The protein expression level was determined as the average of the three or four quantitative values. A ratio dot product, defined as the normalized dot product of the light transition peak areas with the heavy transition peak areas, was equal to 1.0 (an exact match). The protein expression, quantified using the peptides for which signal peaks were obtained at only two or one transition(s), was considered as under the limit of quantification (ULQ). The limit of quantification was determined as the lowest concentration of a stable isotope-labelled peptide for which signal peaks were obtained at three or four transitions. Data were acquired using the Agilent MassHunter Workstation Acquisition software (Agilent Technologies, Data Acquisition for Triple Quad., version B.03.01) and processed with Skyline software (version 4.1). The expression levels of target proteins in crude membranes of isolated rat brain microvessels and brain cortical tissue were expressed as absolute values.

2.8. Western blot analysis

Isolated brain medium-sized vessels from WT and TgF344-AD were weighed and diluted in tissue lysis buffer (50 mM Tris, pH 7.4, 1 mM EDTA, 1% SDS, protease inhibitor cocktail) at a 1:10 tissue weight/lysis buffer volume ratio. Samples were then sonicated and total protein sample content determined by using the Pierce BCA Protein Assay Kit (Thermo Fisher Scientific) according to the manufacturer's recommendations. Samples were aliquoted and stored at −80 °C until the analysis.

Total protein (25 μg) from each sample was mixed with Laemli electrophoresis loading buffer (1 M Tris-HCl, pH 6.8; 20% sodium dodecyl sulphate; 0.4 μL/mL glycerol; 2 g/L bromophenol blue and 2 M dithiothreitol) and resolved in 18% acrylamide gels through SDS-PAGE. Proteins were transferred into nitrocellulose membranes for 90 min at a constant current of 400 mA. Membranes were then blocked in PBS-0.1% Tween 20–5% skimmed milk for 1 h and then incubated overnight with primary antibodies against GAPDH (1:5000; rabbit polyclonal Cat# NB300–327, Novusbio) and mouse monoclonal IC16 antibody recognizing residues 1–16 of the human Aβ (1:500) (Jager et al., 2009) diluted in PBS-0.1% Tween 20–5% skimmed milk. Then, membranes were washed 3 times for 10 min with PBS-0.1% Tween 20 and incubated with HRP-linked secondary antibody goat anti-rabbit (1:5000; Cat# 111–035-144, Jackson ImmunoResearch Labs) and with HRP-linked secondary antibody goat anti-mouse (1:5000; Cat# 074–1806, KPL Kirkegaard & Perry Labs) for 90 min at RT and visualized by Western Lightning Plus-ECL (Enhanced ChemiLuminescence Substrate; PerkinElmer). Images were acquired with a Biorad Chemidoc imager and densitometric analysis was performed by using Biorad Image Lab software (Version 5.1).

2.9. Immunofluorescence staining

Isolated brain microvessels were mounted on microscope slides and fixed with 4% paraformaldehyde in phosphate buffer for 20 min. Specific sites were blocked with PBS-0.1% Triton X-100 and 5% bovine serum albumin (BSA; Sigma-Aldrich) for 1 h at room temperature. Samples were incubated overnight at 4 °C with primary antibodies against collagen IV (1:250; Cat # 1340–01, Southern Biotech) and $A\beta_{1–16}$ (IC16 antibody; 1:500) all diluted in PBS-0.1% Triton X-100 and 2.5% BSA. Then, the samples were washed 3× for 10 min with PBS-0.1% Triton X-100 and incubated with donkey anti-goat IgG Alexafluor 488 (1:1000; Abcam; Cat# ab150129) and goat anti-mouse IgG Alexafluor 555 (1:500; Thermo Fisher; Cat# A21422) all diluted in PBS-0.1% Triton X-100 and 2.5% BSA for 2 h. Finally, the microscope slides were washed, and the capillaries were coverslipped with mounting medium. Negative controls were incubated in the absence of a primary antibody. The images were acquired with Leica TCS SP5 confocal microscope using a 63× water immersion objective.

2.10. Statistical analysis

The absolute protein expression levels are presented as mean ± standard deviation (SD) as well as a ratio of protein expression between WT and TgF344-AD rats. Statistical significance of differences in protein expression between WT and TgF344-AD rats was analysed by unpaired *t*-test. Statistical significance of sex-specific changes in protein expression between male and female WT and TgF344-AD rats was analysed by two-way ANOVA followed by Turkey's multiple comparisons post hoc test (when appropriate) to examine main genotype, sex and genotype*sex interaction effects between WT and TgF344-AD rats. A *p*-value of less than 0.05 was considered to be statistically significant. Data analysis was done using GraphPad Prism, version 5.03 (GraphPad Software, San Diego, CA).

3. Results

3.1. Characterization of the TgF344-AD rat model

The rat model of familial AD, TgF344-AD, was extensively characterized previously (Cohen et al., 2013). In this study, we confirm the presence of Aβ pathology and inflammation in the brain cortical tissue of investigated TgF344-AD rats. The levels of total $A\beta_{1–40}$ and $A\beta_{1–42}$ in the brain cortical tissue of TgF344-AD rats were 0.76 ± 0.015 μg/g brain cortical tissue and 0.75 ± 0.017 μg/g brain cortical tissue, respectively (Fig. 1a). As expected, $A\beta_{1–40}$ and $A\beta_{1–42}$ were not detected in the brain cortical tissues of WT rats (ULQ < 1.56 pg/mL for $A\beta_{1–42}$ and ULQ < 7.81 pg/mL for $A\beta_{1–40}$). In addition, the mRNA expression of inflammation markers, such as COX2, and inflammatory cytokines Il1a and Il1b were significantly increased in the brain cortical tissue of TgF344-AD rats compared to WT controls (Fig. 1b–d). The Aβ levels and mRNA expression of inflammation markers in female and male rats were

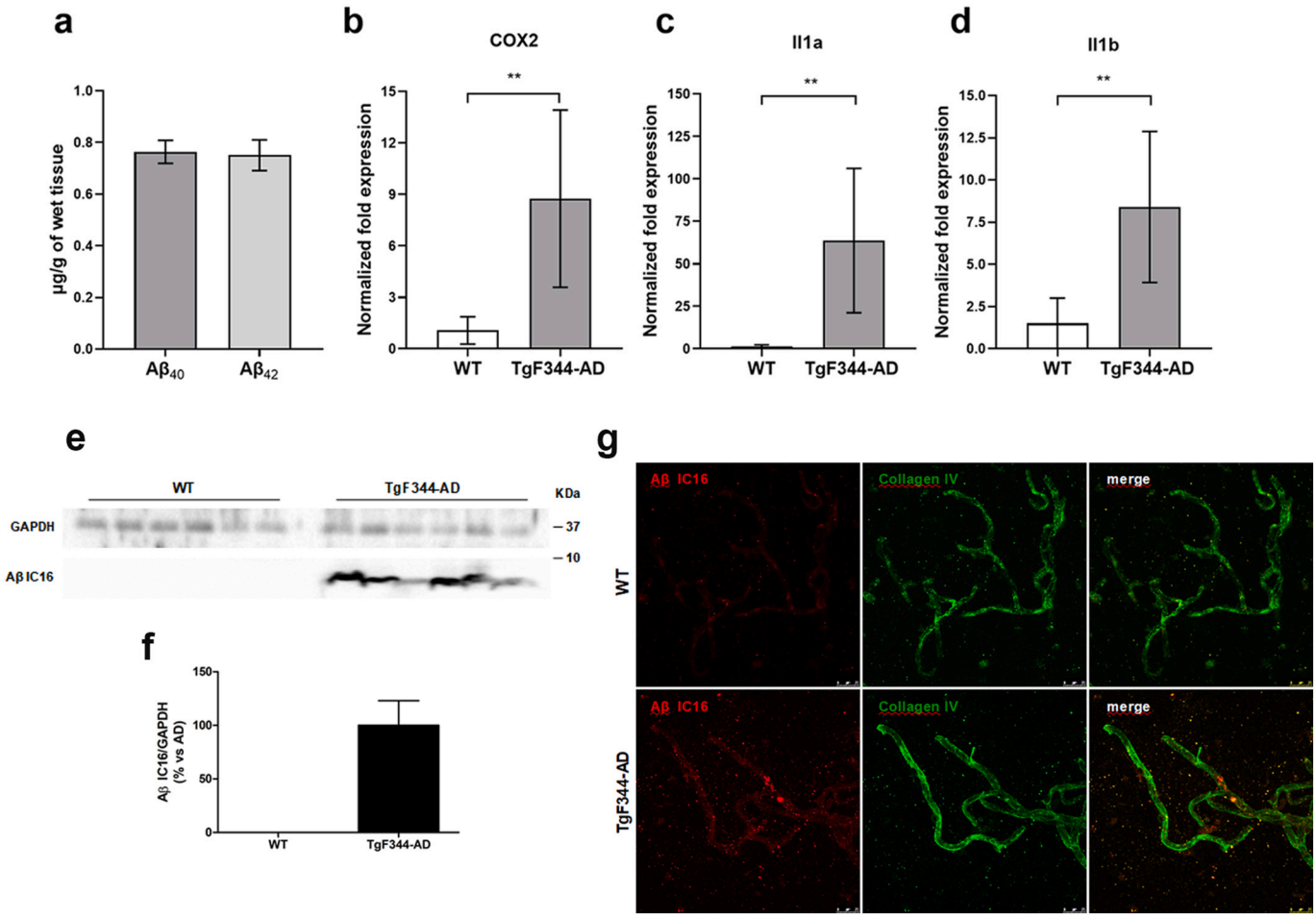

Fig. 1. (a) The total levels of brain cortical $A\beta_{1-40}$ and $A\beta_{1-42}$ in TgF344-AD rats ($n = 10$). The data are present as mean ± SEM. (b-d) Comparison of gene expression of cyclooxygenase-2 (COX2), Interleukins-1 alpha (Il1a) and 1 beta (Il1b) in the brain cortical tissue of the TgF344-AD rats ($n = 9$) and wild-type (WT) rats (n = 9). The data are present as mean ± SD. The gene expression was normalized against the glyceraldehyde-3-phosphate dehydrogenase (Gapdh) house-keeping gene. Statistical significance of changes in protein expression between groups were analysed by unpaired *t*-test (**$p < 0.005$). (e-f) Western Blot and relative densitometry of Aβ IC16 expression in medium-sized vessels isolated from WT and TgF344-AD rat brain cortices. Data are shown as the ratio between Aβ IC16 and GADPH as reference loading control. Each bar represents the mean ± SEM ($n = 6$ per group). (g) Microvessels isolated from WT and TgF344-AD rat brain cortices were immunolabeled with collagen IV antibody to specifically detect cerebral microvessels (green) and Aβ - IC16 antibody (red) to identify fibrillar amyloid. 63 × magnification, scale bar = 25 µm. (For interpretation of the references to colour in this figure legend, the reader is referred to the web version of this article.)

comparable. In addition, the accumulation of Aβ in the isolated brain medium-sized vessels and microvessels was demonstrated in TgF344-AD by western blot (Fig. 1e–f) and immunofluorescence staining analysis (Fig. 1g). These results indicate that TgF344-AD rats used in the study developed CAA, which is in accordance with the previous study by Cohen et al. (2013)(Cohen et al., 2013).

3.2. *Changes in transporter protein expression in the isolated brain microvessels*

The absolute protein expression levels of ABC and SLC transporters were measured in crude membrane fraction of the isolated brain microvessels of WT and TgF344-AD rats (Table 2, Table S2). The comparable purity of the brain microvessel preparations was demonstrated as the protein expression of the endothelial cell marker γ-Gtp was similar in the isolated brain microvessels in both study groups (Table 2), while in the corresponding brain cortical tissues, the protein expression was lower than 0.03 fmol/µg total protein (ULQ). In addition, the enrichment and purity of the isolated brain microvessels were confirmed microscopically and by comparing the normalized gene expression of the brain parenchymal cell markers, i.e. Gfap, Syp, Pdgfrb and endothelial cell marker Pecam1 in isolated brain microvessels versus corresponding brain cortical tissue (Appendix A, Fig. S1, S2). The results (Fig. S2) demonstrated that the isolated microvessels from fresh rat brains represent a combination of the cells and cell fragments including the brain capillary ECs, pericytes and some fraction of astrocytes. In addition, protein expression of the plasma membrane marker Na^+/K^+-ATPase was quantified in the isolated brain microvessels in both study groups at not significantly different levels (Table 2). Thus, the enrichment of the extracted membrane fraction was comparable between the samples, and the observed differences in the protein expression levels of the transporters were not due to the variation in the purity of the extracted membrane fraction.

The study revealed more than three times higher mean protein expression levels of Abcg2 (Bcrp) in the isolated brain microvessels of TgF344-AD rats compared to WT animals ($p = 0.01$) (Table 2, Fig. 2a). The comparison of the Abcc1 (Mrp1) protein expression between the study groups demonstrated twice higher protein expression of the transporter in TgF344-AD rats compared to WT animals ($p = 0.0002$) (Table 2, Fig. 2a). The mean protein expression of Abca1 (Cerp) was 2.8-fold higher in the TgF344-AD rats compared to WT animals, although the difference was not statistically significant ($p = 0.09$) (Table 2, Fig. 2a). For other ABC transporters, i.e. Abcb1 (Mdr1) and Abcc4 (Mrp4), no significant differences in the mean protein expression levels

Table 2
Protein expression levels of SLC and ABC transporters (fmol/μg total protein) in crude membrane fraction of the isolated brain microvessels in wild-type (WT) rats (n = 6) and TgF344-AD rats (n = 6) as well as comparison to protein expression levels in plasma membrane of the isolated brain microvessels in AD patients (n = 5) versus non-demented (ND) individuals (n = 12) (Al-Majdoub et al., 2019).

Protein name/gene name	Isolated brain microvessels in the present study				Isolated brain microvessels (Al-Majdoub et al., 2019)	
	WT rats Mean ± SD	TgF344-AD rats Mean ± SD	Ratio TgF344-AD to WT	p-value	ND individuals Mean ± SD	AD patients Mean ± SD
ABC transporters						
Abcb1/Abcb1	1.6 ± 0.52	2.2 ± 0.61	1.3	0.1	2.6 ± 0.93	2.3 ± 1.5
Abcg2/Abcg2	0.12 ± 0.040	0.37 ± 0.18	3.1	0.01	2.2 ± 0.61	1.9 ± 0.84
Abcc1/Abcc1	0.021 ± 0.007	0.041 ± 0.004	2.0	<0.01	<0.050 (ULQ)	<0.060 (ULQ)
Abcc4/Abcc4	0.046 ± 0.025	0.052 ± 0.034	1.1	0.7	NQ	NQ
Abca1/ Abca1	0.012 ± 0.009[a]	0.033 ± 0.022	2.8	0.09	NQ	NQ
SLC transporters						
ASCT1/Slc1a4	0.17 ± 0.10	0.20 ± 0.18	1.2	0.7	NQ	NQ
GLUT1/Slc2a1	19.0 ± 7.6	20.0 ± 6.5	1.1	0.7	22.0 ± 9.8	18.0 ± 13.0
4F2hc/Slc3a2	0.43 ± 0.22	0.42 ± 0.24	1.0	0.9	NQ	NQ
CAT-1/Slc7a1	0.49 ± 0.21	0.53 ± 0.12	1.1	0.7	NQ	NQ
LAT1/Slc7a5	<0.020 (ULQ)	<0.020 (ULQ)			0.59 ± 0.15	0.56 ± 0.14
MCT1/Slc16a1	<0.10 (ULQ)	<0.10 (ULQ)			5.4 ± 3.7	3.1 ± 1.3
RFC/ Slc19a1	<0.15 (ULQ)	<0.15 (ULQ)			NQ	NQ
OATP1A4/ Slco1a4[b]	<0.015 (ULQ)	<0.015 (ULQ)			0.54 ± 0.10	0.47 ± 0.11
OATP1C1/ Slco1c1	0.13 ± 0.040	0.11 ± 0.080	0.85	0.7	0.27 ± 0.030	0.26 ± 0.040
OCT1/ Slc22a1	<0.15 (ULQ)	<0.15 (ULQ)			0.58 ± 0.11	0.44 ± 0.090
OAT3/ Slc22a8	0.086 ± 0.053	0.089 ± 0.038	1.1	0.9	0.24 ± 0.030	0.24 ± 0.010
FATP1/ Slc27a1	0.051 ± 0.038	0.22 ± 0.13	4.3	0.01	NQ	NQ
ENT1/ Slc29a1	0.027 ± 0.018	0.020 ± 0.012	0.74	0.5	0.22 ± 0.090	0.24 ± 0.040
Endothelial marker, luminal membrane						
γ-Gtp	0.61 ± 0.12	0.71 ± 0.11	1.1	0.2	NQ	NQ
Plasma membrane marker, abluminal						
Na^+/K^+-ATPase	15.0 ± 6.8	19.0 ± 4.1	1.3	0.2	17.0 ± 16.0	22.0 ± 28.0

Data are expressed as mean ± SD. Statistical significance of the changes in protein expression between groups was analysed by unpaired t-test.
NQ - not quantified, as not investigated in the study; ULQ - under limit of quantification.
[a] Abca1 protein expression was quantified in five isolated brain microvessel samples in WT rats, while in one sample the acceptable number of fragment ions of corresponding peptides were not detected.
[b] OATP1A4 is an ortholog of human OATP1A2.

between the TgF344-AD and WT rats were observed (Table 2, Fig. 2a).

The mean protein expression of Fatp1 was significantly higher (4.3-fold) in the isolated brain microvessels of TgF344-AD rats compared to WT animals (p = 0.01). The mean protein expression levels of other SLC transporters, i.e. ASCT1, GLUT1, OATP1C1, OAT3, CAT-1, ENT1, and heavy chain subunit 4F2hc did not differ between the study groups (Table 2, Fig. 1a). Protein expression of LAT1, MCT1, RFC, OATP1A4, OCT1 were below the limits of the quantification, as the acceptable number of fragment ions for corresponding peptides were not detected (Table 2).

3.3. Changes in transporter protein expression in the brain cortical tissue

The absolute protein expression levels of the transporters in the crude membrane fractions of the rat brain cortical tissue were measured and presented in Table 3 and Table S3.

As the total volume of the brain ECs in the brain accounts approximately 0.1% (Pardridge, 2020), we assumed that the transporter protein expression quantified in the brain cortical tissues represents the expression in the brain parenchymal cells, and the impact of the BBB transporter expression is negligible and does not reflect on the observed changes in the brain cortices. The protein expression levels of the plasma membrane marker Na^+/K^+-ATPase did not show statistically significantly difference between the study groups (Table 3) indicating comparable enrichment of the isolated membrane fraction from the sample.

In the brain cortical tissue, no differences in the quantified ABC and SLC transporters were observed while comparing combined protein expression of male and female TgF344-AD rats and WT rats (Table 3, Fig. 2b). However, a two-way ANOVA comparison of protein expression between the male and female TgF344-AD and WT rats revealed a statistically significant interaction between the effects of genotype and sex for 4F2hc ($F(1,21) = 5.9$, p = 0.01), Abcc1 (Mrp1) ($F(1,23) = 7.2$, p = 0.009). Simple main effects analysis showed that gender had a statistically significant effect on the brain cortical protein expression of Abcc1 (Mrp1) in rats (p = 0.01). In male TgF344-AD rats, the protein expression of Abcc1 (Mrp1) in the brain cortical tissue was significantly increased compared to male WT animals (p = 0.01), while no changes were observed in female rats (Fig. 3a). Similarly, a significantly higher protein expression of 4F2hc was observed in male TgF344-AD rats compared to WT rats, while no differences were found in female TgF344-AD and WT rats (Fig. 3b). There were no sex-specific changes in protein expression of Abcb1 (Mdr1), Abcg2 (Bcrp), Abca1 (Cerp), ASCT1, GLUT1, LAT1, FATP1, OATP1C1 in the brain cortical tissue of the TgF344-AD rats compared to WT rats. The protein expression levels of Abcc4 (Mrp4), MCT1, CAT-1, RFC, OCT1, OAT3, ENT1 were below the limit of quantification in the brain cortical samples of both study groups (Table 2).

3.4. Comparison of the changes in transporter protein expression levels in the isolated brain capillaries in AD patients and across the animal models

In this study, changes in absolute protein expression observed in TgF344-AD rat model were compared to those previously reported data in AD patients and animal models. At present, there are three quantitative reports of absolute protein expression of the transporters in AD: two studies in AD patients and our previous report of the transporter expression in the brain cortical tissue of the transgenic mouse APdE9 model (Al-Majdoub et al., 2019; Puris et al., 2021; Storelli et al., 2021).

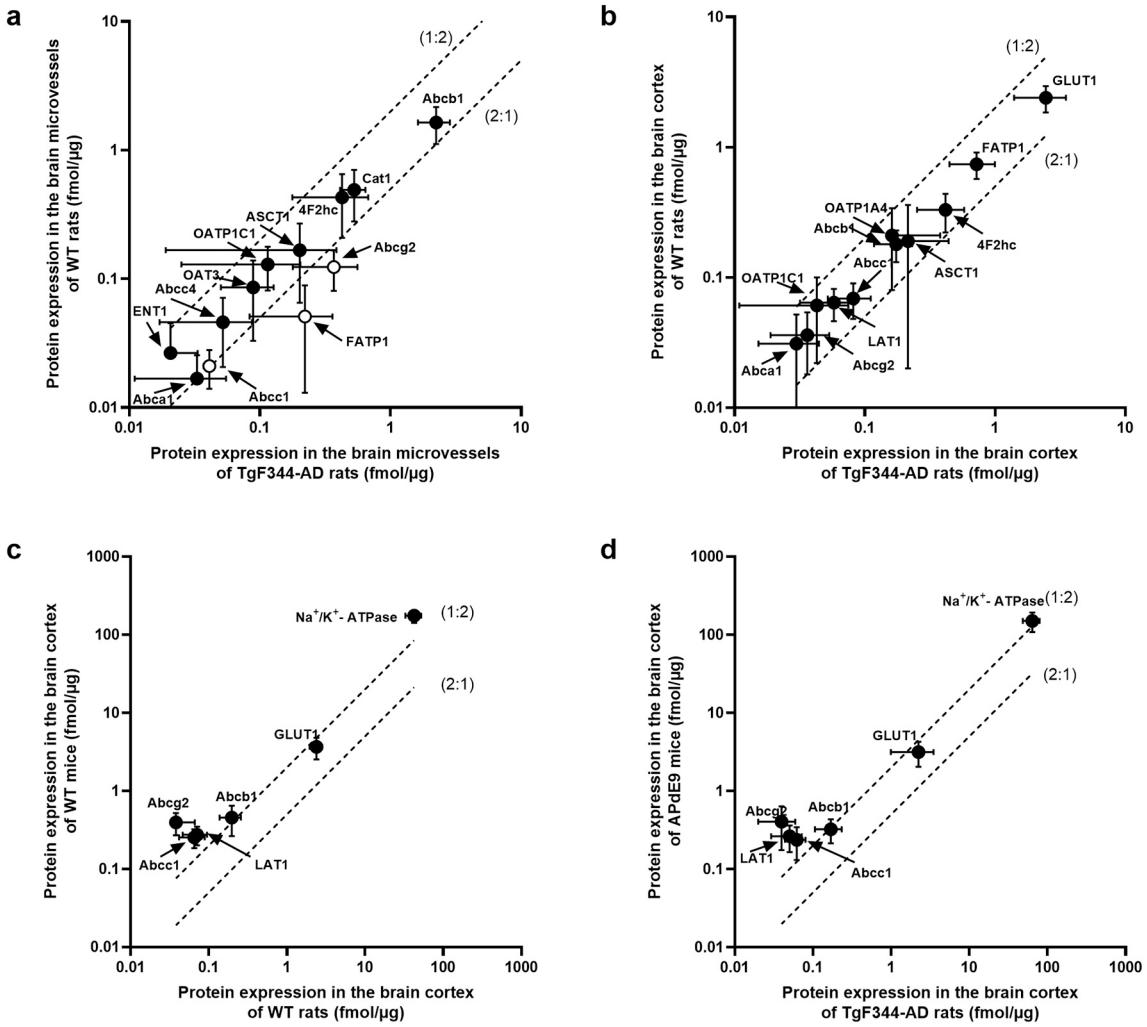

Fig. 2. Comparison of protein expression levels of the transporters in the crude membrane fraction of: (a) the isolated brain microvessels of WT rats (n = 6) versus TgF344-AD rats (n = 6), (b) the brain cortices of WT rats ($n = 13$) versus TgF344-AD rats ($n = 14$), (c) the brain cortices of female WT mice ($n = 5$) versus female WT rats (n = 5), (d) the brain cortices of female APdE9 mice ($n = 4$) versus female TgF344-AD rats ($n = 8$) (Puris et al., 2021). The top and bottom dashed lines represent a 2-fold upregulation or downregulation in protein expression, respectively, between the studied groups. Data are presented as mean ± SD.

The comparison of our findings to the transporter protein expression reported by Storelli et al. (2021) was not possible, as the authors used normalisation by GLUT1 expression to correct the variation in the enrichment of the isolated microvessels in the samples assuming the selective expression of GLUT1 at the BBB (Storelli et al., 2021). However, this and previous studies provide solid evidence that GLUT1 is expressed in the cerebral parenchyma, e.g. in astrocyte cell bodies and processes, as well as in astrocytic end feet surrounding the BBB, and the transporter expression in the brain parenchyma and the BBB can be altered differently (Ding et al., 2013; Gynther et al., 2018; Morgello et al., 1995; Yu and Ding, 1998). Therefore, we compared the absolute protein expression levels in the isolated brain microvessels between rats (WT vs. TgF344-AD) and humans (AD patients vs. non-demented individuals) reported by Al-Majdoub et al. (2019) as shown in Table 2 (Al-Majdoub et al., 2019). In addition, we compared the changes in absolute protein expression of the transporters in the brain cortical tissue of TgF344-AD rat model to those observed in transgenic APdE9 mice, which, similarly to rats, overexpress the human APP_{sw} and PS1ΔE9 mutations (Puris et al., 2021) as compared to WT animals (Table 3, Fig. 2c,d).

At first sight, the brain capillary absolute protein expression of the majority of the transporters was lower in rats (both WT and TgF344-AD) compared to humans (Table 2). However, although the plasma membrane marker expression was comparable between species, the direct comparison and evaluation of statistically significant rat-human differences in the expression of the transporters was not possible due to discrepancies in the methods used for membrane isolation in the studies. Therefore, we compared the changes in transporter expression in isolated brain microvessels between the species in order to evaluate the relevance of the TgF344-AD rat model to mimic the alterations observed in AD patients. Similar to AD patients, there were no changes in Abcb1/ABCB1, GLUT1, OAT3, OATP1C1, ENT1 expression in the isolated brain microvessels of TgF344-AD rats compared to controls (Table 2). Surprisingly, the altered cerebral microvacular expression in Abcg2/ABCG2 observed in TgF344-AD rats was not shown in AD patients compared to non-demented individuals (Table 2). The protein expression levels of other transporters were below the limit of quantification or were not investigated in one of the studies used for the comparison.

The comparison of changes in transporter protein expression in the brain cortical tissue of two animal AD models, TgF344-AD rats and APdE9 mice, revealed no alterations in protein expression of Abcb1 (Mdr1), Abcg2 (Bcrp), Abcc1 (Mrp1), LAT1 and GLUT1 compared to the respective WT controls (Table 3). It should be noted that the comparison was done for female animals, as transporter expression in mouse AD model has been reported for females. The protein expression levels of

Table 3
Protein expression levels of SLC and ABC transporters in crude membrane fraction of the brain cortical tissue of wild-type (WT) rats ($n = 13$) and TgF344-AD rats ($n = 14$) as well as the comparison to the protein expression levels in crude membrane of the brain cortices in transgenic APdE9 mice ($n = 4$) versus age-matched WT ($n = 5$) mice (Puris et al., 2021).

Protein name/gene name	Brain cortical tissue in the present study				Brain cortical tissue (Puris et al., 2021)	
	WT rats Mean ± SD (fmol/µg protein)	TgF344-AD rats Mean ± SD (fmol/µg protein)	Ratio TgF344-AD to WT	*p*-value	WT mice (fmol/µg protein)	APdE9 mice (fmol/µg protein)
ABC transporters						
Abcb1/ Abcb1	0.18 ± 0.049	0.17 ± 0.056	0.94	0.7	0.49 ± 0.19	0.31 ± 0.10
Abcg2/ Abcg2[a]	0.036 ± 0.018	0.034 ± 0.016	0.94	0.8	0.40 ± 0.12	0.32 ± 0.070
Abcc1/ Abcc1	0.069 ± 0.021	0.081 ± 0.029	1.1	0.3	0.27 ± 0.070	0.24 ± 0.11
Abcc4/ Abcc4	<0.010 (ULQ)	<0.010 (ULQ)			0.020 ± 0.010	0.030 ± 0.010
Abca1/ Abca1[a]	0.031 ± 0.021	0.028 ± 0.015	0.90	0.7	NQ	NQ
SLC transporters						
ASCT1/ Slc1a4	0.19 ± 0.17	0.21 ± 0.22	1.1	0.8	NQ	NQ
GLUT1/ Slc2a1	2.4 ± 0.55	2.4 ± 1.0	1.0	0.9	3.7 ± 1.1	3.1 ± 1.1
4F2hc/ Slc3a2	0.33 ± 0.11	0.42 ± 0.16	1.3	0.1	NQ	NQ
CAT-1/ Slc7a1	<0.15 (ULQ)	<0.15 (ULQ)			NQ	NQ
LAT1/ Slc7a5	0.064 ± 0.018	0.058 ± 0.026	0.91	0.5	0.25 ± 0.070	0.26 ± 0.10
MCT1/ Slc16a1	<0.10 (ULQ)	<0.10 (ULQ)			NQ	NQ
RFC/ Slc19a1	<0.15 (ULQ)	<0.15 (ULQ)			NQ	NQ
OATP1A4/ Slco1a4[a]	0.21 ± 0.13	0.15 ± 0.12	0.63	0.4	NQ	NQ
OATP1c1/ Slco1c1	0.061 ± 0.039	0.039 ± 0.028	0.64	0.1	NQ	NQ
OCT1/ Slc22a1	<0.15 (ULQ)	<0.15 (ULQ)			NQ	NQ
OAT3/ Slc22a8	<0.15 (ULQ)	<0.15 (ULQ)			NQ	NQ
FATP1/ Slc27a1	0.74 ± 0.17	0.72 ± 0.27	0.97	0.8	NQ	NQ
ENT1/ Slc29a1	<0.01 (ULQ)	<0.01 (ULQ)			NQ	NQ
Plasma membrane marker						
Na^+/K^+-ATPase	51.0 ± 14.0	57.0 ± 19.0	1.1	0.3	170 ± 33.0	150 ± 42.0

Data are expressed as mean ± SD. Statistical significance of the changes in protein expression between groups was analysed by unpaired *t*-test.
NQ - not quantified, as not investigated in the study; ULQ - under limit of quantification.
[a] Abcg2, Abca1, OATP1A4 protein expression levels were quantified in the brain cortical tissue of WT (n = 13 – Abcg2; $n = 10$ – Abca1; $n = 6$ – OATP1A4) and TgF344-AD ($n = 11$ – Abcg2; n = 11 – Abca1; n = 6 - OATP1A4) rats.

other transporters were below the limit of quantification or were not investigated in one of the studies used for the comparison. Interestingly, the comparison of the absolute protein expression levels between mice and rats, both WT and transgenic AD models, showed more than 2-fold higher protein expression of Abcg2 (Bcrp), Abcc1 (Mrp1), LAT1, Na^+/K^+-ATPase and Abcb1 (Mdr1) (only WT) in mice compared to rats (Fig. 1c,d), which cannot be explained by differences in membrane isolation procedure, as the same methodology and analysis was used in both studies. The differences in expression levels of Abcb1 (Mdr1) (AD models) and GLUT1 (both WT and AD models) were within 2-fold range of the changes (Fig. 2c,d).

4. Discussion

ABC and SLC transporters expressed at the brain barriers may play a significant role in AD, and their expression and/or function can be altered in AD. However, there is a lack of information about quantitative changes in transporter expression and function in the NVU cells in AD patients and animal models. Therefore, there is urgent need for investigation of the changes in transporter protein expression in AD and characterization of the animal models in terms of these changes for their optimal use during drug development.

In the present study, we quantified ABC and SLC transporter protein expression in isolated brain microvessels and brain cortical tissues of the rat AD model and age-matched WT rats, and compared the findings to previous reports in AD patients and animal models. We combined several unique study designs that have not been incorporated in previous reports. First, we used rat model of familial AD, such as TgF344-AD rats, which was characterized in terms of Aβ pathology, CAA and inflammation in this and previous studies, and demonstrated to be more relevant model of AD compared to the mouse models expressing the same mutant human transgenes (Cohen et al., 2013). Second, this is the first report of AD-related changes in transporter expression in both the isolated brain microvessels and the brain cortical tissue investigated in the same animals. Third, we evaluated for the first time sex-specific changes in transporter expression in the brain cortical tissue in AD. Finally, we quantified absolute protein expression of the transporters using the state-of-the-art LC-MS/MS-based QTAP approach providing high selectivity, sensitivity, and reproducibility (Aebersold et al., 2013).

The study revealed more than three times higher protein expression of Abcg2 (Bcrp) in the isolated brain microvessels in TgF344-AD rats compared to WT controls, while expression in the brain cortical tissue of TgF344-AD rats did not differ from that in WT animals. ABCG2/Abcg2 is an efflux transporter, which is expressed at the brain endothelial cells as well as pericytes, astrocytes and microglia, mediating the cellular efflux of sulfoconjugated organic anions and hydrophobic and amphiphilic drugs with significant overlap in substrate specificity with ABCB1/Abcb1 (Pereira et al., 2018). Several studies showed that ABCG2/Abcg2 plays a role in AD via transporting $A\beta_{1-40}$ across the BBB (Do et al., 2012; Xiong et al., 2009; Zhang et al., 2013); preventing generation of reactive-oxygen species (ROS) and consequent activation of the ROS responsive transcription factor NF-κB, which results in decreased expression of inflammatory genes (Shen et al., 2010). Interestingly, absolute protein expression of ABCG2 in isolated brain capillaries was the same in AD patients and non-demented individuals (Al-Majdoub et al., 2019). However, similar to our findings, Xiong et al. (2009) revealed significantly higher BCRP protein expression in the brain microvessels of AD patients with CAA compared to age-matched non-demented subjects using immunohistochemical and western blot analysis, while ABCG2 protein expression in AD patients without CAA did not differ from non-demented controls (Xiong et al., 2009). As TgF344-AD rat model is characterized by CAA, one of the explanations of the observed changes in Abcg2 protein expression in the isolated brain microvessels of TgF344-AD rats can be accumulation of Aβ in the cerebral vessels of this model. Similarly to this study, we did not observe changes in Abcg2 expression in the brain cortical tissue of transgenic APdE9 mice (Puris et al., 2021). Future studies are required to investigate the mechanisms underlying the up-regulation of Abcg2 selectively at the brain microvessels. In addition, as the transporter plays an important role in drug delivery, the overexpression of ABCG2 at the brain microvessels can result in lower extent of brain delivery of drugs, which can lead to reduced pharmacological response in AD patients.

Interestingly, the protein expression of another important efflux pump, Abcb1 (Mdr1), was not altered in both isolated brain microvessels

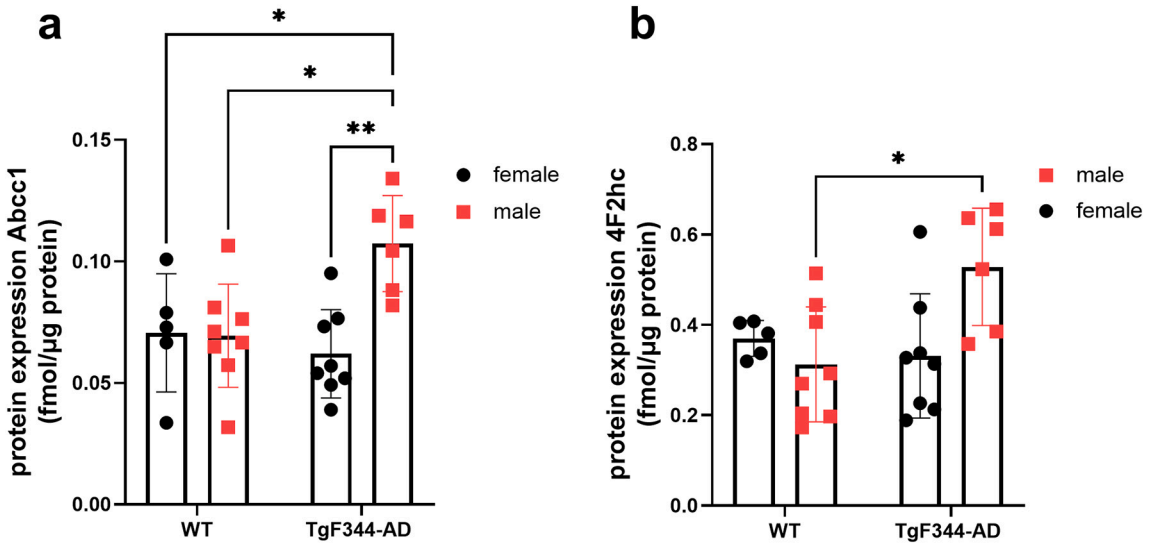

Fig. 3. Sex-specific changes in the protein expression of Abcc1 (Mrp1) (a) and 4F2hc (b) in the brain cortices of wild-type (WT) rats (n = 5 female, n = 8 male) and TgF344-AD rats (n = 8 female, n = 6 male). Data are presented as mean ± SD. Statistical significance of changes in protein expression between groups were analysed by two-way ANOVA followed by Tukey's multiple comparisons test. An asterisk denotes statistical significance between groups (*$p < 0.05$, **$p < 0.01$).

and the brain cortical tissue of the TgF344-AD rats compared to WT animals. ABCB1/Abcb1 is expressed at the brain capillary ECs, pericytes, astrocytes and neurons and thought to be a key player in AD pathogenesis (Pereira et al., 2018). ABCB1/Abcb1 mediates Aβ clearance across the luminal side of the BBB to systemic circulation, and its reduced expression and function at the BBB was found to be associated with Aβ accumulation (Hartz et al., 2010; van Assema et al., 2012; Wijesuriya et al., 2010). However, the quantitative study of the absolute protein expression of ABCB1 in isolated brain capillaries from AD patients and non-demented subjects did not show difference between groups, being in accordance with our findings (Al-Majdoub et al., 2019). Moreover, similar to TgF344-AD rats, in the transgenic APdE9 mice, Mdr1 expression in the brain cortical tissue was not altered as compared to WT controls (Puris et al., 2021). Previous studies in knockout mouse and in vitro models pointed to a compensatory and cooperative role of ABCG2/Abcg2 and ABCB1/Abcb1 at the BBB (Jani et al., 2014; Robinson et al., 2019). Thus, one can suggest that the overexpression of Abcg2 observed in the isolated brain microvessels in TgF344-AD rats could be a compensatory mechanism occurring in order to increase the clearance of Aβ from the brain. Future studies are needed to shed light on a possible cooperative role of ABCG2/Abcg2 and ABCB1/Abcb1 in AD.

Protein expression of Abcc1 (Mrp1) in the isolated brain microvessels of TgF344-AD rats was twice higher compared to WT rats. The transporter is expressed at the brain capillary ECs, pericytes, astrocytes, and neurons (Pereira et al., 2018). Studies in mice suggest the potential involvement of Abcc1 in Aβ clearance from the brain to blood across the BBB (Hofrichter et al., 2013; Krohn et al., 2011). The relative expression of ABCC1 was not altered in isolated brain microvessels of AD patients compared to non-demented controls (Al-Majdoub et al., 2019). Therefore, further studies are required to investigate whether the increase in absolute Abcc1 protein expression in the isolated brain microvessels of the rat AD model is a compensatory mechanism, which might occur in order to facilitate the clearance of Aβ from the brain in addition to Abcg2 up-regulation. Interestingly, in the brain cortical tissue, Abcc1 transporter protein expression was significantly (1.5-fold) up-regulated in male TgF344-AD rats compared to the WT male. These changes were not observed in female TgF344-AD rats, as well as in female transgenic APdE9 mice compared to female WT controls (Puris et al., 2021). The mechanisms underlying the sex-specific changes in Abcc1 expression in AD are unknown and need to be elucidated in future studies.

Protein levels of Abcc4, which are expressed at the brain capillary ECs, astrocytes and microglia (Pereira et al., 2018), were not different in the isolated brain microvessels of TgF344-AD rats and WT controls. The transporter plays a role in the inflammation process, which accompanies AD, by mediating the transport of prostaglandins PGE_2 and PGD_2 into the brain extracellular space where they bind to the corresponding receptors and induce the proinflammatory effects (Reid et al., 2003). Changes in protein expression of the transporter at the NVU in AD have not been reported. Wijesuriya et al. (2010) demonstrated significantly higher ABCC4 protein levels in lysates of hippocampal sections from AD brains compared to non-demented ones using western blot analysis (Wijesuriya et al., 2010). In transgenic APdE9 mice, we did not observe the alterations in protein expression of Abcc4 in the brain cortical tissue (Puris et al., 2021). In this study, transporter expression levels in the rat brain cortical tissue were under quantification limits, and should be investigated in the future.

Another ABC transporter, which is expressed in brain capillary ECs, astrocytes, oligodendrocytes, microglia and neurons, is an ABCA1/Abca1 (CERP/Cerp) (Jani et al., 2014). The changes in absolute protein expression of ABCA1/Abca1 at the brain capillary ECs and other NVU cells in AD have not been previously studied. Here, the expression of Abca1 in the isolated brain microvessels was 2.8-fold higher (not statistically significant) in TgF344-AD rats compared to WT controls. Abca1 protein expression in the brain cortical tissue was similar between the study groups. A potential role of ABCA1/Abca1 in AD is based on functional studies of the transporter, which includes the efflux of cholesterol and phospholipid to enable apoprotein E (ApoE) lipidation, while ApoE is regarded as a chaperone for Aβ, affecting its clearance and aggregation (Boehm-Cagan et al., 2016). Impaired cholesterol metabolism in the brain have been considered to be a risk factor in AD pathogenesis, as cholesterol levels are associated with production of Aβ and high β- and γ-secretase activities in AD brains compared to non-demented controls (Feringa and van der Kant, 2021; Varma et al., 2021; Xiong et al., 2008). Wahrle et al. (2008) demonstrated increased ApoE lipidation and decreased Aβ deposition in the brain of mice overexpressing Abca1 (Wahrle et al., 2008). Our findings highlight the importance of investigation of the transporter at the NVU of AD patients.

A significant (4.3-fold) increase in protein expression of FATP1 in the isolated brain microvessels was observed in TgF344-AD rats compared to WT animals, while no differences were found in the brain cortical tissue. FATP1 is expressed at the brain capillary ECs, neurons and glia,

and mediates the ATP-dependent import of long-chain fatty acids into the cells and also exhibits acyl-CoA ligase activity for long-chain and very-long-chain fatty acids (Liu et al., 2017; Mitchell et al., 2011; Shawahna et al., 2011). The changes in expression of the transporter in AD patients and animal models have not been investigated. However, there is growing evidence that FATP1 is involved in AD pathogenesis. Thus, in the plasma membrane of in vitro BBB model, immortalized human brain capillary ECs (hCMEC/D3), FATP1 protein expression was significantly decreased (by 96.0%) after incubation with $A\beta_{25–35}$, which resulted in diminished transport of its substrate, unesterified docosahexaenoic acid (DHA), from the hCMEC/D3 cells (Ochiai et al., 2019). DHA is an abundant polyunsaturated fatty acid in the human brain, which is essential for maintenance of cognitive function (Yurko-Mauro et al., 2015). The reduction of DHA in the brain has been shown to contribute to AD development (Astarita et al., 2010). Future studies should investigate whether the up-regulation of FATP1 expression in the isolated rat brain microvessels observed in the present study is aimed at increasing the transport of DHA from blood to the brain in order to maintain the DHA levels in the AD brain.

The expression of the investigated amino acid transporters CAT-1, ASC1 as well as LAT1 light (encoded by Slc7a5) and heavy chain 4F2hc (encoded by Slc3a2) subunits in the isolated brain microvessels (except LAT1) and brain cortical tissues (except CAT-1) of TgF344-AD rats did not differ from that in WT animals. All these proteins play an important role in regulating the transport of amino acids across the BBB, and the cell membrane of the brain parenchymal cells (Kasai et al., 2011; Puris et al., 2020; Stoll et al., 1993). Surprisingly, a closer look at the sex-specific changes in protein expression pointed to significant (1.7-fold) up-regulation of heavy chain subunit 4F2hc in male TgF344-AD rats compared to male WT, but not in female rats. 4F2hc is a glycoprotein, which is coupled with the light chain functional subunits (SLC7A5, SLC7A8, etc.) and acts as a molecular chaperone localizing the light chain subunit at the plasma membrane (Verrey et al., 2000). The expression and function of this protein in AD has not been investigated. Thus, our study revealed intriguing differences in 4F2hc protein expression in the brain cortical tissue between male and female AD vs. WT rats, which deserve further study.

The protein expressions of other SLC transporters, such as GLUT1, OAT3, ENT1 and OATP1C1, in the isolated brain microvessels of TgF344-AD rats were similar to those in WT animals. This is in accordance with the findings in AD patients, i.e., not altered levels in these transporters in the isolated brain microvessels in AD patients compared to non-demented individuals (Al-Majdoub et al., 2019). Similarly, there were no changes in protein expression of GLUT1, OATP1C1, OATP1A4 (an ortholog of human OATP1A2) in the brain cortical tissue of TgF344-AD rats compared to WT animals. Likewise, in transgenic APdE9 mice, the protein expression of GLUT1 in the brain cortical tissue was not altered compared to WT mice (Puris et al., 2021).

The limitations of the study need to be acknowledged. First, the sex-specific changes in transporter protein expression in the brain cortical tissue representing the combination of the brain parenchymal cells need to be further investigated in individual brain parenchymal cell populations. In addition, due to the limited sample size, sex-specific changes in the protein expression of the transporters in isolated brain microvessels have not been examined in the present study. Therefore, future research will address this issue. Second, one should remember that the changes observed in the isolated brain microvessels represent alterations in combination of the NVU cells and not only endothelial cells. Third, despite the technological progress over the past decade, there is still potential for improvement in the field of LC-MS/MS-based proteomics applied to quantify very low abundance proteins. Finally, the characterization of the investigated AD rats was performed in terms of Aβ pathology, CAA and inflammation, all of which can impact the transporter expression at the BBB (Kania et al., 2011; Varatharaj and Galea, 2017). Future studies should focus on determination of the specific molecular mechanisms underlying the changes in transporter protein expression observed in the present study.

5. Conclusions

In conclusion, absolute protein expression levels of ABC and SLC transporters in the isolated brain microvessels and the brain cortical tissue of rat TgF344-AD model and age-matched WT controls were quantified using LC-MS/MS-based QTAP approach. The study revealed significant up-regulation of Abcg2 (Bcrp), Abcc1 (Mrp1) and FATP1 in the isolated brain microvessels of the TgF344-AD rats indicating potential involvement of these transporters in AD pathogenesis. The changes in transporter protein expression in the isolated brain microvessels and the brain cortical tissue were different indicating of various transporter expression regulation mechanisms in the cells comprised of these tissues in AD. Moreover, we investigated for the first time sex-specific changes in protein expression of the transporters in the rat brain cortical tissue. The study revealed male-specific alterations in Abcc1 (Mrp1) and 4F2hc protein expression indicating the potential differences in regulation of their expressions in AD between men and women. These findings highlight the importance of the investigation of sex-specific changes in biochemical perturbations in AD. Finally, TgF344-AD rat model was characterized in terms of the relevance to mimic the changes in transporter expression in AD patients and compared to available data in animal models. The study sheds light not only on the potential role of transporters in molecular mechanisms underlying AD, but on the rational use of animal models for drug candidate testing and evaluation of drug delivery in AD.

Funding

This study was supported by the Alexander von Humboldt Foundation (awarded to Elena Puris), the Alzheimer Forschung Initiative e.V. (International Training Grant awarded to Elena Puris), as well as the Biocenter Finland and Biocenter Kuopio supporting the analytical chemistry laboratory. We acknowledge support from Alzheimer Forschung Initiative e.V. for Open Access Publishing.

CRediT authorship contribution statement

Elena Puris: Conceptualization, Methodology, Validation, Formal analysis, Investigation, Resources, Data curation, Writing – original draft, Writing – review & editing, Visualization, Supervision, Project administration, Funding acquisition. **Seppo Auriola:** Methodology, Investigation, Resources, Writing – review & editing. **Sabrina Petralla:** Formal analysis, Investigation, Writing – review & editing, Visualization. **Robin Hartman:** Investigation, Writing – review & editing. **Mikko Gynther:** Methodology, Investigation, Resources, Writing – review & editing. **Elizabeth C.M. de Lange:** Conceptualization, Methodology, Resources, Writing – review & editing. **Gert Fricker:** Conceptualization, Resources, Writing – review & editing.

Declaration of Competing Interest

None.

Acknowledgements

The authors thank Ms. Miia Reponen (University of Eastern Finland) for technical assistance in analytical chemistry. The authors would like to thank Prof. Claus Pietrzik and Ms. Magdalena Kurtyka, Institute for Pathobiochemistry, University Medical Center of Johannes Gutenberg University Mainz, Mainz, Germany for providing IC16 antibody, as well as Prof. Marco Caprini, Department of Pharmacy and Biotechnology, University of Bologna, Italy for providing the antibody against collagen IV.

Appendix A. Supplementary data

Supplementary data to this article can be found online at https://doi.org/10.1016/j.nbd.2022.105741.

References

Abbott, N.J., Patabendige, A.A., Dolman, D.E., Yusof, S.R., Begley, D.J., 2010. Structure and function of the blood-brain barrier. Neurobiol. Dis. 37, 13–25.

Aebersold, R., Burlingame, A.L., Bradshaw, R.A., 2013. Western blots versus selected reaction monitoring assays: time to turn the tables? Mol. Cell. Proteomics 12, 2381–2382.

Al-Majdoub, Z.M., Al Feteisi, H., Achour, B., Warwood, S., Neuhoff, S., Rostami-Hodjegan, A., Barber, J., 2019. Proteomic quantification of human blood-brain barrier SLC and ABC transporters in healthy individuals and dementia patients. Mol. Pharm. 16, 1220–1233.

Alzheimer's Association, 2016. 2016 Alzheimer's disease facts and figures. Alzheimers Dement. 12, 459–509.

Astarita, G., Jung, K.M., Berchtold, N.C., Nguyen, V.Q., Gillen, D.L., Head, E., Cotman, C. W., Piomelli, D., 2010. Deficient liver biosynthesis of docosahexaenoic acid correlates with cognitive impairment in Alzheimer's disease. PLoS One 5, e12538.

Boehm-Cagan, A., Bar, R., Liraz, O., Bielicki, J.K., Johansson, J.O., Michaelson, D.M., 2016. ABCA1 agonist reverses the ApoE4-driven cognitive and brain pathologies. J. Alzheimers Dis. 54, 1219–1233.

Chai, A.B., Leung, G.K.F., Callaghan, R., Gelissen, I.C., 2020. P-glycoprotein: a role in the export of amyloid-beta in Alzheimer's disease? FEBS J. 287, 612–625.

Cohen, R.M., Rezai-Zadeh, K., Weitz, T.M., Rentsendorj, A., Gate, D., Spivak, I., Bholat, Y., Vasilevko, V., Glabe, C.G., Breunig, J.J., Rakic, P., Davtyan, H., Agadjanyan, M.G., Kepe, V., Barrio, J.R., Bannykh, S., Szekely, C.A., Pechnick, R.N., Town, T., 2013. A transgenic Alzheimer rat with plaques, tau pathology, behavioral impairment, oligomeric abeta, and frank neuronal loss. J. Neurosci. 33, 6245–6256.

Cornford, E.M., Hyman, S., 2005. Localization of brain endothelial luminal and abluminal transporters with immunogold electron microscopy. NeuroRx 2, 27–43.

Czapiga, M., Colton, C.A., 2003. Microglial function in human APOE3 and APOE4 transgenic mice: altered arginine transport. J. Neuroimmunol. 134, 44–51.

Ding, F., Yao, J., Rettberg, J.R., Chen, S., Brinton, R.D., 2013. Early decline in glucose transport and metabolism precedes shift to ketogenic system in female aging and Alzheimer's mouse brain: implication for bioenergetic intervention. PLoS One 8, e79977.

Do, T.M., Noel-Hudson, M.S., Ribes, S., Besengez, C., Smirnova, M., Cisternino, S., Buyse, M., Calon, F., Chimini, G., Chacun, H., Scherrmann, J.M., Farinotti, R., Bourasset, F., 2012. ABCG2- and ABCG4-mediated efflux of amyloid-beta peptide 1-40 at the mouse blood-brain barrier. J. Alzheimers Dis. 30, 155–166.

Dobryakova, Y.V., Volobueva, M.N., Manolova, A.O., Medvedeva, T.M., Kvichansky, A. A., Gulyaeva, N.V., Markevich, V.A., Stepanichev, M.Y., Bolshakov, A.P., 2019. Cholinergic deficit induced by central administration of 192IgG-saporin is associated with activation of microglia and cell loss in the dorsal hippocampus of rats. Front. Neurosci. 13, 146.

Erickson, M.A., Banks, W.A., 2013. Blood-brain barrier dysfunction as a cause and consequence of Alzheimer's disease. J. Cereb. Blood Flow Metab. 33, 1500–1513.

Feringa, F.M., van der Kant, R., 2021. Cholesterol and Alzheimer's disease; from risk genes to pathological effects. Front. Aging Neurosci. 13, 690372.

Ferretti, M.T., Iulita, M.F., Cavedo, E., Chiesa, P.A., Schumacher Dimech, A., Santuccione Chadha, A., Baracchi, F., Girouard, H., Misoch, S., Giacobini, E., Depypere, H., Hampel, H., Women's Brain, P., the Alzheimer Precision Medicine, I, 2018. Sex differences in Alzheimer disease - the gateway to precision medicine. Nat. Rev. Neurol. 14, 457–469.

Filon, J.R., Intorcia, A.J., Sue, L.I., Vazquez Arreola, E., Wilson, J., Davis, K.J., Sabbagh, M.N., Belden, C.M., Caselli, R.J., Adler, C.H., Woodruff, B.K., Rapscak, S.Z., Ahern, G.L., Burke, A.D., Jacobson, S., Shill, H.A., Driver-Dunckley, E., Chen, K., Reiman, E.M., Beach, T.G., Serrano, G.E., 2016. Gender differences in Alzheimer disease: brain atrophy, histopathology burden, and cognition. J. Neuropathol. Exp. Neurol. 75, 748–754.

Furst, A.J., Lal, R.A., 2011. Amyloid-beta and glucose metabolism in Alzheimer's disease. J. Alzheimers Dis. 26 (Suppl. 3), 105–116.

Gao, S., Hendrie, H.C., Hall, K.S., Hui, S., 1998. The relationships between age, sex, and the incidence of dementia and Alzheimer disease: a meta-analysis. Arch. Gen. Psychiatry 55, 809–815.

Guo, B., Zhou, Q., 2018. How efficient are rodent models for Alzheimer's disease drug discovery? Expert Opin. Drug Discovery 13, 113–115.

Guo, T., Zhang, D., Zeng, Y., Huang, T.Y., Xu, H., Zhao, Y., 2020. Molecular and cellular mechanisms underlying the pathogenesis of Alzheimer's disease. Mol. Neurodegener. 15, 40.

Gynther, M., Proietti Silvestri, I., Hansen, J.C., Hansen, K.B., Malm, T., Ishchenko, Y., Larsen, Y., Han, L., Kayser, S., Auriola, S., Petsalo, A., Nielsen, B., Pickering, D.S., Bunch, L., 2017. Augmentation of anticancer drug efficacy in murine hepatocellular carcinoma cells by a peripherally acting competitive N-methyl-d-aspartate (NMDA) receptor antagonist. J. Med. Chem. 60, 9885–9904.

Gynther, M., Puris, E., Peltokangas, S., Auriola, S., Kanninen, K.M., Koistinaho, J., Huttunen, K.M., Ruponen, M., Vellonen, K.S., 2018. Alzheimer's disease phenotype or inflammatory insult does not alter function of L-type amino acid transporter 1 in mouse blood-brain barrier and primary astrocytes. Pharm. Res. 36, 17.

Hartz, A.M., Miller, D.S., Bauer, B., 2010. Restoring blood-brain barrier P-glycoprotein reduces brain amyloid-beta in a mouse model of Alzheimer's disease. Mol. Pharmacol. 77, 715–723.

Heneka, M.T., Carson, M.J., El Khoury, J., Landreth, G.E., Brosseron, F., Feinstein, D.L., Jacobs, A.H., Wyss-Coray, T., Vitorica, J., Ransohoff, R.M., Herrup, K., Frautschy, S. A., Finsen, B., Brown, G.C., Verkhratsky, A., Yamanaka, K., Koistinaho, J., Latz, E., Halle, A., Petzold, G.C., Town, T., Morgan, D., Shinohara, M.L., Perry, V.H., Holmes, C., Bazan, N.G., Brooks, D.J., Hunot, S., Joseph, B., Deigendesch, N., Garaschuk, O., Boddeke, E., Dinarello, C.A., Breitner, J.C., Cole, G.M., Golenbock, D. T., Kummer, M.P., 2015. Neuroinflammation in Alzheimer's disease. Lancet Neurol. 14, 388–405.

Hofrichter, J., Krohn, M., Schumacher, T., Lange, C., Feistel, B., Walbroel, B., Heinze, H. J., Crockett, S., Sharbel, T.F., Pahnke, J., 2013. Reduced Alzheimer's disease pathology by St. John's Wort treatment is independent of hyperforin and facilitated by ABCC1 and microglia activation in mice. Curr. Alzheimer Res. 10, 1057–1069.

Hoshi, Y., Uchida, Y., Tachikawa, M., Inoue, T., Ohtsuki, S., Terasaki, T., 2013. Quantitative atlas of blood-brain barrier transporters, receptors, and tight junction proteins in rats and common marmoset. J. Pharm. Sci. 102, 3343–3355.

Jager, S., Leuchtenberger, S., Martin, A., Czirr, E., Wesselowski, J., Dieckmann, M., Waldron, E., Korth, C., Koo, E.H., Heneka, M., Weggen, S., Pietrzik, C.U., 2009. Alpha-secretase mediated conversion of the amyloid precursor protein derived membrane stub C99 to C83 limits Abeta generation. J. Neurochem. 111, 1369–1382.

Jani, M., Ambrus, C., Magnan, R., Jakab, K.T., Beery, E., Zolnerciks, J.K., Krajcsi, P., 2014. Structure and function of BCRP, a broad specificity transporter of xenobiotics and endobiotics. Arch. Toxicol. 88, 1205–1248.

Jia, Y., Wang, N., Zhang, Y., Xue, D., Lou, H., Liu, X., 2020. Alteration in the function and expression of SLC and ABC transporters in the neurovascular unit in Alzheimer's disease and the clinical significance. Aging Dis. 11, 390–404.

Kadry, H., Noorani, B., Cucullo, L., 2020. A blood-brain barrier overview on structure, function, impairment, and biomarkers of integrity. Fluids Barriers CNS 17, 69.

Kania, K.D., Wijesuriya, H.C., Hladky, S.B., Barrand, M.A., 2011. Beta amyloid effects on expression of multidrug efflux transporters in brain endothelial cells. Brain Res. 1418, 1–11.

Kasai, Y., Tachikawa, M., Hirose, S., Akanuma, S., Hosoya, K., 2011. Transport systems of serine at the brain barriers and in brain parenchymal cells. J. Neurochem. 118, 304–313.

Krohn, M., Lange, C., Hofrichter, J., Scheffler, K., Stenzel, J., Steffen, J., Schumacher, T., Bruning, T., Plath, A.S., Alfen, F., Schmidt, A., Winter, F., Rateitschak, K., Wree, A., Gsponer, J., Walker, L.C., Pahnke, J., 2011. Cerebral amyloid-beta proteostasis is regulated by the membrane transport protein ABCC1 in mice. J. Clin. Invest. 121, 3924–3931.

Laws, K.R., Irvine, K., Gale, T.M., 2018. Sex differences in Alzheimer's disease. Curr. Opin. Psychiatry. 31, 133–139.

Liu, L., MacKenzie, K.R., Putluri, N., Maletic-Savatic, M., Bellen, H.J., 2017. The glia-neuron lactate shuttle and elevated ROS promote lipid synthesis in neurons and lipid droplet accumulation in glia via APOE/D. Cell Metab. 26 (719–737), e716.

Liu, X., Hou, D., Lin, F., Luo, J., Xie, J., Wang, Y., Tian, Y., 2019. The role of neurovascular unit damage in the occurrence and development of Alzheimer's disease. Rev. Neurosci. 30, 477–484.

Lyros, E., Bakogiannis, C., Liu, Y., Fassbender, K., 2014. Molecular links between endothelial dysfunction and neurodegeneration in Alzheimer's disease. Curr. Alzheimer Res. 11, 18–26.

Malpetti, M., Ballarini, T., Presotto, L., Garibotto, V., Tettamanti, M., Perani, D., Alzheimer's Disease Neuroimaging Initiative, d, Network for, E., Standardization of Dementia Diagnosis, d, 2017. Gender differences in healthy aging and Alzheimer's dementia: a (18) F-FDG-PET study of brain and cognitive reserve. Hum. Brain Mapp. 38, 4212–4227.

Mehta, D., Jackson, R., Paul, G., Shi, J., Sabbagh, M., 2017. Why do trials for Alzheimer's disease drugs keep failing? A discontinued drug perspective for 2010-2015. Expert Opin. Investig. Drugs 26, 735–739.

Menaceur, C., Gosselet, F., Fenart, L., Saint-Pol, J., 2021. The blood-brain barrier, an evolving concept based on technological advances and cell-cell communications. Cells 11.

Mitchell, R.W., On, N.H., Del Bigio, M.R., Miller, D.W., Hatch, G.M., 2011. Fatty acid transport protein expression in human brain and potential role in fatty acid transport across human brain microvessel endothelial cells. J. Neurochem. 117, 735–746.

Morgello, S., Uson, R.R., Schwartz, E.J., Haber, R.S., 1995. The human blood-brain barrier glucose transporter (GLUT1) is a glucose transporter of gray matter astrocytes. Glia 14, 43–54.

Oakley, H., Cole, S.L., Logan, S., Maus, E., Shao, P., Craft, J., Guillozet-Bongaarts, A., Ohno, M., Disterhoft, J., Van Eldik, L., Berry, R., Vassar, R., 2006. Intraneuronal beta-amyloid aggregates, neurodegeneration, and neuron loss in transgenic mice with five familial Alzheimer's disease mutations: potential factors in amyloid plaque formation. J. Neurosci. 26, 10129–10140.

Ochiai, Y., Uchida, Y., Tachikawa, M., Couraud, P.O., Terasaki, T., 2019. Amyloid beta25-35 impairs docosahexaenoic acid efflux by down-regulating fatty acid transport protein 1 (FATP1/SLC27A1) protein expression in human brain capillary endothelial cells. J. Neurochem. 150, 385–401.

Ohtsuki, S., Uchida, Y., Kubo, Y., Terasaki, T., 2011. Quantitative targeted absolute proteomics-based ADME research as a new path to drug discovery and development: methodology, advantages, strategy, and prospects. J. Pharm. Sci. 100, 3547–3559.

Pan, Y., Omori, K., Ali, I., Tachikawa, M., Terasaki, T., Brouwer, K.L.R., Nicolazzo, J.A., 2018. Altered expression of small intestinal drug transporters and hepatic metabolic enzymes in a mouse model of familial Alzheimer's disease. Mol. Pharm. 15, 4073–4083.

Pan, Y., Omori, K., Ali, I., Tachikawa, M., Terasaki, T., Brouwer, K.L.R., Nicolazzo, J.A., 2019. Increased expression of renal drug transporters in a mouse model of familial Alzheimer's disease. J. Pharm. Sci. 108, 2484–2489.
Pardridge, W.M., 2020. The isolated Brain microvessel: a versatile experimental model of the blood-brain barrier. Front. Physiol. 11, 398.
Peinnequin, A., Mouret, C., Birot, O., Alonso, A., Mathieu, J., Clarencon, D., Agay, D., Chancerelle, Y., Multon, E., 2004. Rat pro-inflammatory cytokine and cytokine related mRNA quantification by real-time polymerase chain reaction using SYBR green. BMC Immunol. 5, 3.
Pereira, C.D., Martins, F., Wiltfang, J., da Cruz, E.S.O.A.B., Rebelo, S., 2018. ABC transporters are key players in Alzheimer's disease. J. Alzheimers Dis. 61, 463–485.
Puris, E., Gynther, M., de Lange, E.C.M., Auriola, S., Hammarlund-Udenaes, M., Huttunen, K.M., Loryan, I., 2019. Mechanistic study on the use of the l-type amino acid transporter 1 for brain intracellular delivery of ketoprofen via prodrug: a novel approach supporting the development of prodrugs for intracellular targets. Mol. Pharm. 16, 3261–3274.
Puris, E., Gynther, M., Auriola, S., Huttunen, K.M., 2020. L-type amino acid transporter 1 as a target for drug delivery. Pharm. Res. 37, 88.
Puris, E., Auriola, S., Korhonen, P., Loppi, S., Kanninen, K.M., Malm, T., Koistinaho, J., Gynther, M., 2021. Systemic inflammation induced changes in protein expression of ABC transporters and ionotropic glutamate receptor subunit 1 in the cerebral cortex of familial Alzheimer's disease mouse model. J. Pharm. Sci. 110, 3953–3962.
Reid, G., Wielinga, P., Zelcer, N., van der Heijden, I., Kuil, A., de Haas, M., Wijnholds, J., Borst, P., 2003. The human multidrug resistance protein MRP4 functions as a prostaglandin efflux transporter and is inhibited by nonsteroidal antiinflammatory drugs. Proc. Natl. Acad. Sci. U. S. A. 100, 9244–9249.
Robinson, N., Grabowski, P., Rehman, I., 2018. Alzheimer's disease pathogenesis: is there a role for folate? Mech. Ageing Dev. 174, 86–94.
Robinson, A.N., Tebase, B.G., Francone, S.C., Huff, L.M., Kozlowski, H., Cossari, D., Lee, J.M., Esposito, D., Robey, R.W., Gottesman, M.M., 2019. Coexpression of ABCB1 and ABCG2 in a cell line model reveals both independent and additive transporter function. Drug Metab. Dispos. 47, 715–723.
Roostaei, T., Nazeri, A., Felsky, D., De Jager, P.L., Schneider, J.A., Pollock, B.G., Bennett, D.A., Voineskos, A.N., Alzheimer's Disease Neuroimaging, I, 2017. Genome-wide interaction study of brain beta-amyloid burden and cognitive impairment in Alzheimer's disease. Mol. Psychiatry 22, 287–295.
Shawahna, R., Uchida, Y., Decleves, X., Ohtsuki, S., Yousif, S., Dauchy, S., Jacob, A., Chassoux, F., Daumas-Duport, C., Couraud, P.O., Terasaki, T., Scherrmann, J.M., 2011. Transcriptomic and quantitative proteomic analysis of transporters and drug metabolizing enzymes in freshly isolated human brain microvessels. Mol. Pharm. 8, 1332–1341.
Shen, S., Callaghan, D., Juzwik, C., Xiong, H., Huang, P., Zhang, W., 2010. ABCG2 reduces ROS-mediated toxicity and inflammation: a potential role in Alzheimer's disease. J. Neurochem. 114, 1590–1604.
Stoll, J., Wadhwani, K.C., Smith, Q.R., 1993. Identification of the cationic amino acid transporter (System y+) of the rat blood-brain barrier. J. Neurochem. 60, 1956–1959.
Storelli, F., Billington, S., Kumar, A.R., Unadkat, J.D., 2021. Abundance of P-glycoprotein and other drug transporters at the human blood-brain barrier in Alzheimer's disease: a quantitative targeted proteomic study. Clin. Pharmacol. Ther. 109, 667–675.
Sweeney, M.D., Kisler, K., Montagne, A., Toga, A.W., Zlokovic, B.V., 2018. The role of brain vasculature in neurodegenerative disorders. Nat. Neurosci. 21, 1318–1331.
Taylor, S.C., Nadeau, K., Abbasi, M., Lachance, C., Nguyen, M., Fenrich, J., 2019. The ultimate qPCR experiment: producing publication quality, reproducible data the first time. Trends Biotechnol. 37, 761–774.
Uchida, Y., Ohtsuki, S., Katsukura, Y., Ikeda, C., Suzuki, T., Kamiie, J., Terasaki, T., 2011. Quantitative targeted absolute proteomics of human blood-brain barrier transporters and receptors. J. Neurochem. 117, 333–345.
Uchida, Y., Tachikawa, M., Obuchi, W., Hoshi, Y., Tomioka, Y., Ohtsuki, S., Terasaki, T., 2013. A study protocol for quantitative targeted absolute proteomics (QTAP) by LC-MS/MS: application for inter-strain differences in protein expression levels of transporters, receptors, claudin-5, and marker proteins at the blood-brain barrier in ddY, FVB, and C57BL/6J mice. Fluids Barriers CNS 10, 21.
van Assema, D.M., Lubberink, M., Bauer, M., van der Flier, W.M., Schuit, R.C., Windhorst, A.D., Comans, E.F., Hoetjes, N.J., Tolboom, N., Langer, O., Muller, M., Scheltens, P., Lammertsma, A.A., van Berckel, B.N., 2012. Blood-brain barrier P-glycoprotein function in Alzheimer's disease. Brain 135, 181–189.
Varatharaj, A., Galea, I., 2017. The blood-brain barrier in systemic inflammation. Brain Behav. Immun. 60, 1–12.
Varma, V.R., Busra Luleci, H., Oommen, A.M., Varma, S., Blackshear, C.T., Griswold, M. E., An, Y., Roberts, J.A., O'Brien, R., Pletnikova, O., Troncoso, J.C., Bennett, D.A., Cakir, T., Legido-Quigley, C., Thambisetty, M., 2021. Abnormal brain cholesterol homeostasis in Alzheimer's disease-a targeted metabolomic and transcriptomic study. NPJ Aging Mech. Dis. 7, 11.
Verrey, F., Meier, C., Rossier, G., Kuhn, L.C., 2000. Glycoprotein-associated amino acid exchangers: broadening the range of transport specificity. Pflugers Arch. 440, 503–512.
Wahrle, S.E., Jiang, H., Parsadanian, M., Kim, J., Li, A., Knoten, A., Jain, S., Hirsch-Reinshagen, V., Wellington, C.L., Bales, K.R., Paul, S.M., Holtzman, D.M., 2008. Overexpression of ABCA1 reduces amyloid deposition in the PDAPP mouse model of Alzheimer disease. J. Clin. Invest. 118, 671–682.
Wijesuriya, H.C., Bullock, J.Y., Faull, R.L., Hladky, S.B., Barrand, M.A., 2010. ABC efflux transporters in brain vasculature of Alzheimer's subjects. Brain Res. 1358, 228–238.
Wittmann, G., Szabon, J., Mohacsik, P., Nouriel, S.S., Gereben, B., Fekete, C., Lechan, R. M., 2015. Parallel regulation of thyroid hormone transporters OATP1c1 and MCT8 during and after endotoxemia at the blood-brain barrier of male rodents. Endocrinology 156, 1552–1564.
Xiong, H., Callaghan, D., Jones, A., Walker, D.G., Lue, L.F., Beach, T.G., Sue, L.I., Woulfe, J., Xu, H., Stanimirovic, D.B., Zhang, W., 2008. Cholesterol retention in Alzheimer's brain is responsible for high beta- and gamma-secretase activities and Abeta production. Neurobiol. Dis. 29, 422–437.
Xiong, H., Callaghan, D., Jones, A., Bai, J., Rasquinha, I., Smith, C., Pei, K., Walker, D., Lue, L.F., Stanimirovic, D., Zhang, W., 2009. ABCG2 is upregulated in Alzheimer's brain with cerebral amyloid angiopathy and may act as a gatekeeper at the blood-brain barrier for Abeta(1-40) peptides. J. Neurosci. 29, 5463–5475.
Yu, S., Ding, W.G., 1998. The 45 kDa form of glucose transporter 1 (GLUT1) is localized in oligodendrocyte and astrocyte but not in microglia in the rat brain. Brain Res. 797, 65–72.
Yurko-Mauro, K., Alexander, D.D., Van Elswyk, M.E., 2015. Docosahexaenoic acid and adult memory: a systematic review and meta-analysis. PLoS One 10, e0120391.
Zhang, W., Xiong, H., Callaghan, D., Liu, H., Jones, A., Pei, K., Fatehi, D., Brunette, E., Stanimirovic, D., 2013. Blood-brain barrier transport of amyloid beta peptides in efflux pump knock-out animals evaluated by in vivo optical imaging. Fluids Barriers CNS 10, 13.